



**POLITECNICO**  
MILANO 1863

SCUOLA DI INGEGNERIA INDUSTRIALE  
E DELL'INFORMAZIONE

# A bibliographic review of Pumped Thermal Energy Storage technology based on Brayton cycle

TESI DI LAUREA MAGISTRALE IN  
ENERGY ENGINEERING  
INGEGNERIA ENERGETICA

Author: **Matteo Grande**

Student ID: 944493

Advisor: Marco Astolfi

Academic Year: 2022-23



# Acknowledgements

# Abstract

Pumped Thermal Electricity Storage (PTES) based on a Joule-Brayton cycle is a promising grid-scale energy storage technology, whose working principle is to store electricity in the form of high-grade thermal energy. This thesis provides an overview of the inner workings, operating principle and current development status of the many PTES variants proposed to date in the scientific literature or by manufacturers. The potential and competitiveness of the various candidate designs are quantified and discussed thanks to the definition of specific design parameters. Thermodynamic performance estimates are reported and used to assess the value of this technology as a potential large-scale, long-duration and long-lifetime energy storage option, with unique sector-coupling features and low geographical constraints.

**Key-words:** electricity storage, Pumped Thermal Energy Storage (PTES)

## Abstract in italiano

Il Pumped Thermal Energy Storage (PTES) basato su ciclo Joule-Brayton è una promettente tecnologia di accumulo di energia su larga scala, il cui principio di funzionamento è immagazzinare elettricità sotto forma di energia termica. Questa tesi fornisce una panoramica del principio di funzionamento, dei principali componenti e dello stato di sviluppo attuale delle numerose varianti di PTES proposte fino ad oggi nella letteratura scientifica o dai produttori. Le potenzialità e la competitività dei vari modelli proposti vengono valutate e confrontate grazie alla definizione di specifici parametri progettuali. Le stime delle prestazioni termodinamiche vengono riportate e utilizzate per valutare il valore di questa tecnologia come potenziale opzione di accumulo di energia su larga scala, lunga durata e lunga vita operativa, con caratteristiche uniche di accoppiamento settoriale e bassi vincoli geografici.

**Parole chiave:** Accumulo di energia elettrica, Pumped Thermal Electricity Storage (PTES)



# Contents

<b>Acknowledgements</b> .....	<b>i</b>
<b>Abstract</b> .....	<b>ii</b>
<b>Abstract in italiano</b> .....	<b>iii</b>
<b>Contents</b> .....	<b>v</b>
<b>List of Figures</b> .....	<b>vii</b>
<b>List of Tables</b> .....	<b>ix</b>
<b>1 Introduction</b> .....	<b>10</b>
1.1. Energy storage technology overview .....	11
1.2. Electrical Energy Storage (EES) technologies and their characteristics	12
1.2.1. Thermal energy storage .....	13
1.2.2. Pumpido Hydro Storage .....	14
1.2.3. Compressed Air Energy Storage .....	14
1.2.4. Lithium ion (Li-ion) batteries .....	15
1.2.5. Flow batteries .....	15
1.2.6. Liquid Air Energy Storage.....	15
1.2.7. Hydrogen Energy Storage .....	16
1.2.8. Pumped Thermal Energy Storage .....	16
<b>2 Pumped Thermal Energy Storage: basic concepts</b> .....	<b>19</b>
2.1. PTES working principle .....	19
2.2. Matching of heat sources and heat sinks with realistic power cycles...	21
2.3. Description of PTES with Brayton thermodynamic cycle and main components .....	23
2.4. Rating parameters and notations.....	27
<b>3 Literature review of PTES based on Brayton cycle</b> .....	<b>31</b>
3.1. Main design parameters and variation of performance with operating conditions .....	32
3.2. Historical background.....	37
3.3. Cycle configuration .....	41
3.4. Working fluid selection.....	42
3.5. Thermal storage system configurations .....	44

3.5.1.	Solid storage systems .....	45
3.5.2.	Liquid storage systems .....	51
3.6.	Compression and expansion machinery .....	54
3.6.1.	Reciprocating piston engine .....	56
3.7.	Other components .....	58
3.7.1.	Heat exchangers .....	58
3.7.2.	Buffer vessel .....	58
3.8.	Cost breakdown into components.....	59
3.9.	Integration of PTES systems with other energy sources and sinks .....	60
3.10.	Optimization of system performances .....	62
3.11.	Thermo-economic analysis.....	69
<b>4</b>	<b>Comparisons and final considerations .....</b>	<b>72</b>
	<b>Bibliography .....</b>	<b>75</b>



## List of Figures

- Figure 1.1: Discharge power rating and rated discharge energy capacity for TMES systems. The black diagonal lines represent discharge duration at the given discharge power rating and rated discharge energy capacity [13]. ..... 18
- Figure 2.1: Basic scheme of a PTES system acting as a heat pump during charge (solid line) and as a heat engine during discharge (dashed line) [18]..... 20
- Figure 2.2: Match between the cycle and heat sources/sinks [16]. ..... 21
- Figure 2.3: Generic T-s diagram for ideal Brayton PTES, Transcritical PTES and Latent PTES cycle (left); Comparison for different PTES types based on ideal cycle analysis. Commonly considered working fluids for PTES (argon, air, water, CO<sub>2</sub> and ammonia) were used to derive these numbers (right)..... 22
- Figure 2.4: (a) Basic scheme of a PTES system using solid thermal storage and (b) T-s diagram of ideal cycles developed by SAIPEM and Isentropic Ltd [20]. ..... 24
- Figure 2.5: Layout of a PTES system and corresponding T-s diagram [21]... 24
- Figure 2.6: T-s diagrams for irreversible PTES cycles [22]. ..... 25
- Figure 2.7: (a) Plant layout of an indirect storage recuperated Joule-Brayton PTES system during charge [13]; (b) layout of a direct storage PTES system during charge [22]..... 27
- Figure 3.1: Layout of a PTES system and T-s diagram of the ideal cycle during charge [22]..... 33
- Figure 3.2: Roundtrip efficiency correlations of Brayton-cycle PTES with  $\eta_i = 90\%$ . The points represent data from literature.  $\square$ : SAIPEM design with  $\eta_p = 90\%$  (Desrues et al., 2010).  $\Delta$ : Isentropic design with  $\eta_p = 90\%$  (McTigue, White and Markides, 2015).  $\odot$ : Isentropic design with  $\eta_p = 99\%$  (McTigue, White and Markides, 2015).  $\diamond$  Malta design with  $\eta_p = 90\%$  (Olympios et al., 2021).  $\theta = T_1/T_3$  [13]. ..... 35
- Figure 3.3: The work ratio and heat-to-work ratio can inform the design of PTES systems for  $\eta_i = 90\%$ . The points represent data from the literature. Blue points are work ratios and grey points are heat-to-work ratios.  $\square$ : SAIPEM design (Desrues et al., 2010).  $\Delta$ : Isentropic design with  $\eta_p = 90\%$  (McTigue, White and Markides, 2015).  $\odot$ : Isentropic design with  $\eta_p = 99\%$  (McTigue,

White and Markides, 2015). ♦ Malta design with $\eta_p = 90\%$ (Olympios et al., 2021). $\theta = T_1/T_3$ [13].	36
Figure 3.4: Layout of Ruer PTES system.	38
Figure 3.5: T–s diagrams for Joule-Brayton PTES systems proposed by Isentropic and Saipem.	39
Figure 3.6: Layout of the PTES system proposed by MacNaghten and Howes [29].	40
Figure 3.7: Layout of the PTES system proposed by Laughlin et al. [31].	40
Figure 3.8: Schematic layout of a packed bed. The hot thermal reservoir is orientated vertically during charge. Gas enters at T1 and exits at T2.	46
Figure 3.9: Reservoir temperature profiles for different modes of operation. See [22] for details.	48
Figure 3.10: Layout of a liquid storage PTES system.	51
Figure 3.11: Scheme of a reciprocating device [58].	56
Figure 3.12: Section through working space of first prototype by MacNaghten and Howes [14].	57
Figure 3.13: Valve prototype by MacNaghten and Howes [30].	57
Figure 3.14: Breakdown of the investment cost of a Brayton-cycle PTES system based on packed-bed thermal stores into components for systems designed to provide a rated discharge power of: (a) 1 MW; and (b) 100 MW. Outer and inner rings represent costs for systems designed to have a discharge duration of 72 h and 8 h, respectively.	59
Figure 3.15: Layout of a new solar-PTES plant proposed by Farres-Antunez [60].	60
Figure 3.16: Pareto fronts (trade-off surfaces) from the optimisation by McTigue et al. [21].	64
Figure 3.17: Thermo-economic analysis of two PTES systems based on Joule–Brayton cycle for varying discharge power rating and discharge duration: (a) power capital cost for a system with liquid-tank TES; (b) energy capital cost for a system with liquid-tank TES; (c) power capital cost for a system with packed-bed TES; and (d) energy capital cost for a system with packed-bed TES. The plots are logarithmic on both axes [13].	71

# List of Tables

Table 1.1 Comparison of design parameters for several energy storage technologies. ....	17
Table 3.1: Operating conditions for Joule-Brayton based PTES systems suggested by patents. ....	41
Table 3.2: Main properties of selected working fluid options. $T_{\text{crit}}$ and $p_{\text{crit}}$ represent the critical temperature and pressure, respectively; and MM the molar mass of the fluid.....	42
Table 3.3: Types and characteristics of packed bed storage systems used in literature.....	46
Table 3.4: Main characteristics of sensible heat solid storage materials used in packed beds [54]. ....	50
Table 3.5: Main characteristics of sensible heat liquid storage materials. The values of the thermophysical properties correspond to intermediate temperatures between $T_{\text{min}}$ and $T_{\text{max}}$ [54].....	52
Table 3.6: Summary of different liquid TES configurations proposed in literature.....	54
Table 3.7: Summary of Brayton-cycle PTES models proposed in the literature with key parameters.....	68

# 1 Introduction

In recent years it has become clear that global warming and climate change are directly linked to the raise of greenhouse gasses emission. The International Panel on Climate Change (IPCC) estimates that human activity has caused the increase of the global average temperature of 1,0 °C from preindustrial levels [1]. The Paris Agreement, the first-ever universal, legally binding global climate change agreement, adopted at the Paris climate conference (COP21) in December 2015, sets out a global framework to avoid dangerous climate change by limiting global warming to well below 2°C and pursuing efforts to limit it to 1.5°C [2]. As part of the European Green Deal, the European Commission adopted a set of proposals to make the EU's climate, energy, transport and taxation policies fit for reducing net greenhouse gas emissions by at least 55% by 2030, compared to 1990 levels [3]. Key targets for 2030 are at least 40% cuts in greenhouse gas emissions (from 1990 levels), 32% share for renewable energy and 32.5% improvement in energy efficiency.

Despite rising costs for key materials used to make solar panels and wind turbines, additions of new renewable power capacity this year are forecast to rise to 320 gigawatts (GW) in 2022, surpassing the previous all-time high set in 2021, according to the latest edition of the IEA's annual Renewables Market Report [4]. By 2026, global renewable electricity capacity is forecast to rise more than 60% from 2020 levels to over 4800 GW, which is equivalent to the current total global power capacity of fossil fuels and nuclear combined. Renewable energy sources (RES) are set to account for almost 95% of the increase in global power capacity through 2026, with solar PV alone providing more than half. The amount of renewable capacity added over the period of 2021 to 2026 is expected to be 50% higher than from 2015 to 2020. This is driven by stronger support from government policies and more ambitious clean energy goals, announced before and during the COP26 Climate Change Conference [5].

In order to meet the 2050 net-zero carbon emission (NZE) target it will be required a much higher penetration of renewable sources (RES) into the energy system. Wind, solar, hydro, etc. are environmentally friendly energy sources that guarantee to produce electricity in eco-friendly ways but, unlike the hydroelectric power, wind and solar production suffer of high variability, unpredictability and uncontrollability. These characteristics cause large fluctuations in the daily, monthly or even annually

power production, so this presents a great challenge in energy generation and load balance maintenance to ensure power network stability and reliability of a renewable energy system [6]. This calls for highly flexible, low-cost, energy and resource-efficient storage technologies to balance the energy supply and demand mismatch. A solution to this problem is the employment of electricity storage systems (ESS), which allow to store electricity during the peak of RES generation and feed it back to the grid when there is no RES production.

## 1.1. Energy storage technology overview

Before classifying the available energy storage technologies, it is fundamental to define the energy storage concept. An Energy Storage System (ESS) is a device in which energy can be stored in some form and can be subsequently extracted to perform some useful operation, like reducing imbalances between energy demand and energy production. To store some form of energy, three steps need to be done: charging, storing and discharging. Each step can occur more than one time during each storage cycle and some of the steps can take place simultaneously [7].

The following are some applications of energy storage technologies (ESS):

1. Energy arbitrage: it involves storing electricity at off-peaks when the cost is low and selling it at peak demand periods when the cost is high.
2. Load levelling: it is the utilization of the stored energy at peak periods, reducing the requirements of peaking generators.
3. Renewable integration: storage systems could minimize the effect of intermittency of renewable energy resources and increase their penetration in power grids, thus allowing renewable generation to be dispatched more easily.
4. Spinning reserve: storage systems could reduce the requirement for idling generators in power systems. Such generators are dedicated to 'take over' of any sudden failure of a major generator, but ESSs could defer the option of operating them.
5. Customer-side peak shaving: this involves reliability back-up support by ESSs with the use of uninterruptible power supply (UPS) to address short and long period interruptions.
6. Primary frequency regulation: this involves the provision of frequency stability support for power networks through the charge/discharge characteristics of ESSs, regulating the voltage and frequency.

7. Investment deferral: involves the use of storage to defer transmission and distribution (T/D) infrastructure investment.

Electricity in its form is not storable. The only way through which it can be stored is by converting it into more stable and storable energy forms, with the aim to transform it back to electricity when needed. Various technologies can be used and they are regarded, for example by Aneke and Wang [7], as Electrical Energy Storage (EES) technologies, according to the purpose for which the energy is stored, although there is not a unique way to classify them. Electrical Energy Storage can be sub-classified as follows: Mechanical ES, Chemical ES, Electrochemical ES, Superconducting Magnetic ES (SMES) and Thermal Energy Storage. In Mechanical Energy Storage (MES), electricity is converted into another easy storable form of energy by means of electromechanical systems. MES units include Pumped Hydro Storage, Compressed Air Energy Storage (CAES), Gravity Energy Storage (GES), Liquid Piston Energy Storage (LPES), Liquid Air Energy Storage (LAES), Pumped Thermal Electricity Storage and Flywheels Energy Storage (FES). Hydrogen, methane, hydrocarbons or biofuels like ethanol, methanol biodiesel, etc. are part of the category called Chemical Energy Storage. Supercapacitors, fuel cells and batteries constitute the technologies that compose the Electrochemical Energy Storage systems. Thermal Energy Storage (TES) can be divided in three methods, which are sensible heat, latent heat and thermochemical heat.

In some cases technologies from one category may be integrated with those of another category, for instance thermal stores can be incorporated in CAES technology.

## 1.2. Electrical Energy Storage (EES) technologies and their characteristics

Some useful performance metrics are provided to make a comparison between different storage technologies. The energy density  $q_E$  and power density  $q_P$  are important performance metrics for energy storage systems and give an indication of the scale and economic feasibility of the system. The energy capital cost, which is the total system cost over the rated discharge energy capacity (\$/kWh), and the power capital cost, which is the total system cost over rated discharge power (\$/kW), depend approximately inversely with  $q_E$  and  $q_P$ . The precise definitions of energy and power density vary from author to author and depend on the technology. However, most commonly  $q_E$  is defined as the stored available energy divided by the volume of the

storage media, while  $q_P$  is the energy produced divided the volumetric flow rate of the working fluid. The round-trip of energy storage systems is defined as the ratio of the net work output during discharge to the net work input during charge:

$$RTE = \frac{\text{Net work output}}{\text{Net work input}} = \frac{W_{dis}^{net}}{W_{ch}^{net}} \quad (1.1)$$

### 1.2.1. Thermal energy storage

Thermal energy storage has applications in cooling and refrigeration, solar power plants, solar cooking and seasonal energy storage. It can be divided into three categories: latent heat, sensible heat or thermo-chemical heat.

In the first case, the energy is stored in the latent heat of a storage medium during a constant temperature process, like a phase change. This has several advantages, such as high energy densities and the ability to provide heat at a constant temperature. However, problems include a change in volume associated with the phase change, pinch point constraints and identifying suitable materials. Liquid-vapour transition PCMs require a large volume for the gas storage and generally solid-liquid transitions are preferred.

In sensible heat systems, the heat is stored in the change of storage materials temperature, which is a consequence of a variation in the internal energy. Sensible heat technologies are relatively cheap and simple to manufacture, although they have a lower energy density than latent heat systems.

Water is a popular choice for sensible heat storage, due to its high specific heat capacity and density, chemical inertness and the fact it can be used as both a heat transfer fluid and a storage medium. Water is limited to a certain temperature range unless it is pressurized, therefore for high temperature operation solids are generally preferred. Heat resistant oils can operate in a broader range of temperatures without pressurization than water. Other suitable liquids include molten salts, which have a wide range of operating temperatures and they are nontoxic, non-flammable and are widely used in solar plants. Rocks are a good alternative to liquids since they are cheap, readily available and can operate at high temperatures.

Thermo-chemical heat storage uses reversible exotherm or endotherm chemical reactions with thermo-chemical materials (TCM), which involve the absorption and release of heat for the purpose of thermal energy storage. Heat is applied to decompose certain molecules. The reaction products are then separated, and mixed again when required, resulting in a release of energy. Some examples are the decomposition of potassium oxide (over a range of 300-800 °C), lead oxide (300-350 °C) and calcium

hydroxide [8]. Comprehensive reviews of thermal energy storage materials and technologies can be found in [8].

### 1.2.2. Pumpido Hydro Storage

Pumped Hydro Storage (PHS) or Pumped Hydroelectric Energy Storage is the most mature, commercially available and widely adopted large-scale energy storage technology since the 1890s. This storage technology actually covers 95% of the total world capacity of large-scale energy storage installations [9].

The PHS technology uses gravity to store the electrical energy and a typical plant layout consist of an upper and a lower reservoir, a waterfall, pipes, a pump, a turbine, an electric motor and an electric generator. The pump and the turbine can be separated machines or the same device supplies both the functions. In the second case, the turbomachine is called reversible pump-turbine. Also the electric machine can be unique, like a motor/generator, or made by separated devices.

The basic concept of PHS is really simple. The off-peak power is taken from the grid and used to feed the electric motor, which drives the pump. The water is pumped from the lower to the upper reservoir and stored here. During high demand hours, the water is released from the upper to the lower reservoir through a turbine, which is mechanically coupled with an electric generator.

The major drawback of the PHS technology is related to the need of an acceptable water availability and an adequate geographical morphology. Aspect which increases the capital cost. For these reasons, new PHS units can be installed only in countries with a favourable morphology or upgrading conventional hydroelectric power units.

### 1.2.3. Compressed Air Energy Storage

It is the second commercially available large-scale energy storage technology. The first conceptualization of CAES technology was presented in the early 1940s [10], but the first CAES plant was built 30 years later. As for the working principle of PHS, also the CAES one is really simple. When the power demand is low, excess generation capacity is used to compress the air and store it in an underground cavern (hard rock caverns, salt caverns, depleted gas fields, aquifer, etc.) or in above ground man-made tanks, containers or vessels. During high peak demand hours, the stored and pressurized air is drawn from the storage, heated up, usually using natural gas, and expanded in an air turbine, converting back the potential energy of the pressurized air into electricity. This kind of CAES plant is called Diabatic CAES (D-CAES) because, during the compression phase, the generated heat is wasted, and two plants were built, the Huntorf plant in Germany and the McIntosh plant in the USA [10].



However, Diabatic CAES is an energy storage technology that uses fossil fuel and this implies a non-negligible environmental impact during the discharging phase. Therefore, during the years, the researchers have studied and developed other plant configurations with the aim of reducing fuel consumption, recovering the heat generated during the compression process and mitigating the issue related to the geographical requirements. Adiabatic CAES (ACAES), Isothermal CAES (I-CAES) and Underwater CAES (UW-CAES) are the upgraded versions of the Diabatic CAES.

#### 1.2.4. Lithium ion (Li-ion) batteries

These batteries use lithium metal or lithium compound as anode. The Li-ion batteries are lighter, smaller and more powerful than other batteries, which make it attractive for consumer electronics. Their energy and power density range from 90 to 190 Wh/kg and 500 to 2000 W/kg [7]. They also have high efficiency and low self-discharge rate making it suitable for electric vehicles solutions. Their major drawback is that they are fragile with temperature dependent life cycle. They usually require a special protection circuit to avoid overload. These together with the high capital cost (\$900–1300/kW h) limit their use for large capacity applications.

#### 1.2.5. Flow batteries

Flow batteries are a relatively young technology, which works in a similar manner as conventional batteries. The ions flow from the negative and the positive electrodes during charging and delivering phases respectively through a selective membrane.

The major drawbacks are the poor lifetime (5–15 years) and the high capital costs.

#### 1.2.6. Liquid Air Energy Storage

Liquid Air Energy Storage is another emerging large-scale storage technology, which implies to store electrical energy in the form of liquefied air. As in CAES technology, the first step of the charging phase consists on the air compression. Then, the pressurized air is liquefied and stored in thermally isolated man-made vessels, tanks or containers. During discharge, the liquid air is heated up using a heat exchanger. During this process, the pressure is increased and the high pressure air is used to drive an expansion machine mechanically connected to the electric generator.

The main advantages of LAES are the high energy density, 50Wh/l or 97–210Wh/kg, and the low volume occupied by the liquid air compared to the gaseous one (1/700). This feature guarantees to drastically reduce the storage vessels volume. In fact, a

LAES plant can be up to 12 and up to 140 times smaller than a CAES and a PHS plant, respectively.

Regarding the round-trip efficiency, the actual value is in the range 40–50%, but significant improvements can be achieved when the charging phase waste heat is recovered and used during delivery. In this case, the round-trip efficiency is expected to be in the range between 70% and 85%. Based on available calculation, it is expected that LAES plants can be built with a nameplate power in the range from 0.35 to 100 MW, a storage capacity of 10–1000 MWh and a lifetime of 20–40 years [7].

The main LAES drawback is the high cost: 900–2000 \$/kW and 260–530 \$/kWh. Regarding the response time, it is expected in the range 5–10 min while the self-discharge rate is very small. Although few tests were conducted, based on the demonstration plant built up by Highview Power Storage [11] in Slough (UK), significant technological improvements are expected in the near future.

### 1.2.7. Hydrogen Energy Storage

Hydrogen Energy Storage is the most convenient way to store off-peak electricity when long-term season-to-season storage is needed. During the charging phase, water is transformed in hydrogen using the electrolysis process. The produced hydrogen can be stored in gaseous or liquid form as well as using metal hydrides or carbon nanostructures. When power is needed, the stored hydrogen can be used in a fuel cell or directly burnt in gas turbine.

Several works are available in the scientific literature, but all of them underline the need of developing safer and efficient hydrogen storage system with acceptable volumetric energy densities. It is expected that this technology has a power rate comprised between 0.1 and 1000 MW, a storage capacity in the range 100–1000 MWh, an energy density in the range 500–3000 Wh/l (or 800–10000 Wh/kg), a power density higher than 500 W/kg (or 500 W/l), a round-trip efficiency of 20–50% and a lifetime comprised between 5 and 30 years. The capital costs are expected in the range 1900–10000 \$/kW, while the price per stored energy unit and the price per cycle can be estimated in the range 1–10 \$/kWh and 6000–20000 \$/kWh per cycle, respectively. The expected self-discharge rate is small while the estimated cycle life is approximately equal to 1000 cycles.

### 1.2.8. Pumped Thermal Energy Storage

Pumped Thermal Electricity Storage (PTES) or Pumped Heat Energy Storage is the last in-developing storage technology suitable for large-scale ES applications. PTES is based on a high temperature heat pump cycle, which transforms the off-peak

electricity into thermal energy and stores it inside two man-made thermally isolated vessels: one hot and one cold.

Compared to CAES and PHS, PTES is characterised by higher energy density (110–170 Wh/l or 50–140 Wh/kg), low self-discharge rate (1 %/day). The working fluid is a gaseous medium, air or argon, while electricity is stored as sensible heat using cheap and solid materials like concrete, gravel or other common minerals. Therefore, PTES is characterised by low capital costs: 600 \$/kW and 60 \$/kWh. It does not suffer of low cycle life, like flow batteries, and the expected round-trip efficiency (70–80%) and lifetime (25–30 year) are very good.

In additions, it has no geographical limitations, it is composed of well-known and studied components available in the market today and it has low environmental impact and long lifetime.

The typical storage period of PTESs can cover hours to weeks and like other Thermo-Mechanical Energy Storage (TMES) systems, it can be used to provide thermal energy along with electrical energy during discharging and can be integrated with other heat sources (waste, renewable, high temperature heat and/or cold demand) and power generation systems that involve thermal energy conversion. Moreover, PTES units can be integrated in fossil-fueled thermal power plant to reduce cycling operation, fast start up and overnight shutdowns.

For these reasons and being the power rating and the storage capacity in the range 0,5–10MW (or larger) and 0.5–60 MWh (or larger), the PTES technology has the potential to become a competitive solution in the field of energy storage from the large scale to the small scale [6].

Table 1.1 Comparison of design parameters for several energy storage technologies.

EES	Discharge power [MW]	Energy density [kWh/m <sup>3</sup> ]	Power density [kW/m <sup>3</sup> ]	Power capex [\$/kW]	Energy capex [\$/kWh]	RTE [%]	Oper. lifetime [years]
PHS	100 - 5000	0,5 - 1,5	0,5 - 1,5	600 - 2000	5 - 100	65 - 87	40 - 60
CAES	1 - 300	3 - 6	0,5 - 2	400 - 800	2 - 50	50 - 89	20 - 40
LAES	10 - 200	50	-	900 - 2000	260 - 530	55 - 80	20 - 40

Brayton PTES	10 - 150	20 - 50	1 - 15	1000 - 6000	100 - 500	50 - 75	25 - 30
Li-ion battery	0 - 0,1	200 - 500 (90 - 190 Wh/kg) <sup>1</sup>	1500 - 10000 W/L (500 - 2000 W/kg) <sup>1</sup>	1200 - 4000	600 - 2500	90 - 97	20
VRB flow battery	0,03 - 3	10 - 30	~< 2	600 - 1000	150 - 1000	75 - 85	5 - 10

1. Values taken from Aneke and Wang [7] and Luo et al. [12].

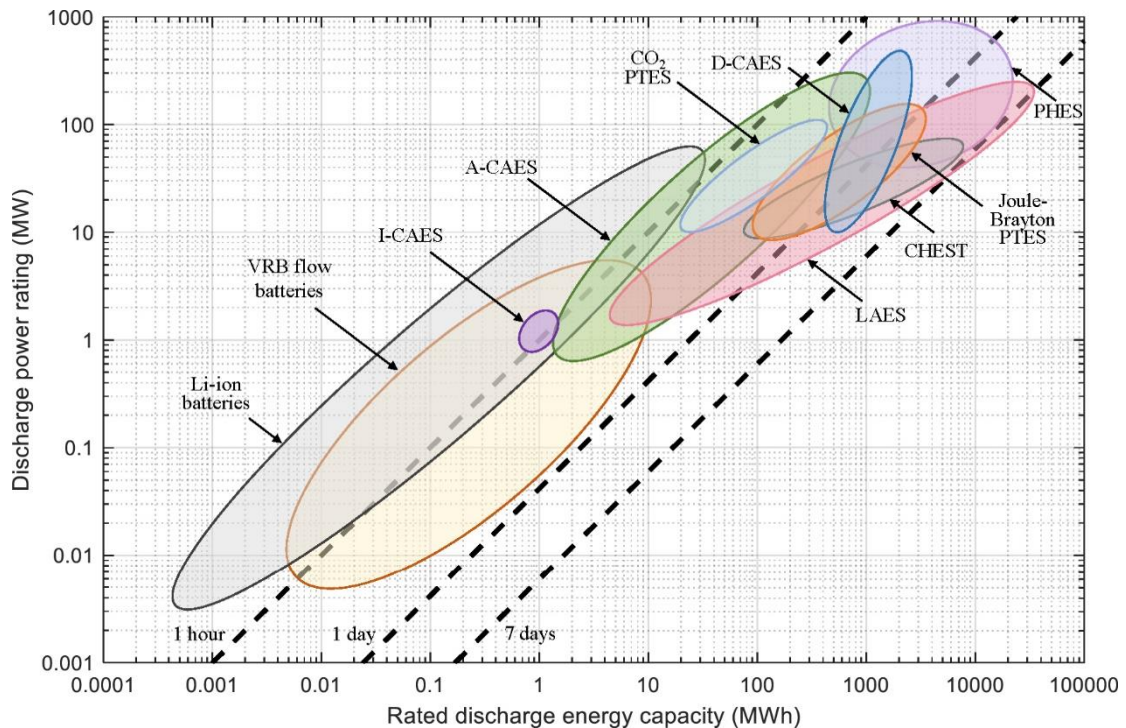


Figure 1.1: Discharge power rating and rated discharge energy capacity for TMES systems. The black diagonal lines represent discharge duration at the given discharge power rating and rated discharge energy capacity [13].

## 2 Pumped Thermal Energy Storage: basic concepts

### 2.1. PTES working principle

Pumped Thermal Energy Storage (PTES) is an energy storage technology that transforms electricity into high-grade thermal energy, stores the heat in two insulated heat reservoirs, and converts the heat back to electricity when required.

A number of variants exists and perhaps the most widely used name is Pumped Heat Energy Storage (PHES) [14], [15], but it is known also with other names as Electrothermal Energy Storage (ETES) [16] and Thermo-electrical energy storage (TEES). It can also be referred with the term Carnot Battery (CB), which is an energy storage solution where charge and discharge processes involve forward and backward conversions, respectively, between electricity and heat, while the storage phase consists of thermal energy storage [17]. The term encompasses also several thermo-mechanical storage concepts, like liquid air energy storage (LAES).

The PTES system follows a ‘reversible’ thermodynamic cycle, based on heat pumps and heat engines. In this case, reversible means that the direction of the gas flow through the heat pump is reversed to begin operation as a heat engine.

A complete working cycle is characterized by two phases: a “charging phase” and a “discharging phase”. During charge, or loading period, the system operates as a heat pump (HP), using electricity to drive a compressor and transfer heat from a colder region to a hotter region, storing high-grade thermal energy in two insulated heat reservoirs, a hot and a cold one. During the delivery, or discharge period, the cycle is reversed and the system operates as a heat engine (HE), so the heat is returned from the hot reservoir (HR) to the cold reservoir (CR), driving an expander and recovering electricity.

A basic scheme of the heat pump/engine cycles is shown in Figure 2.1:

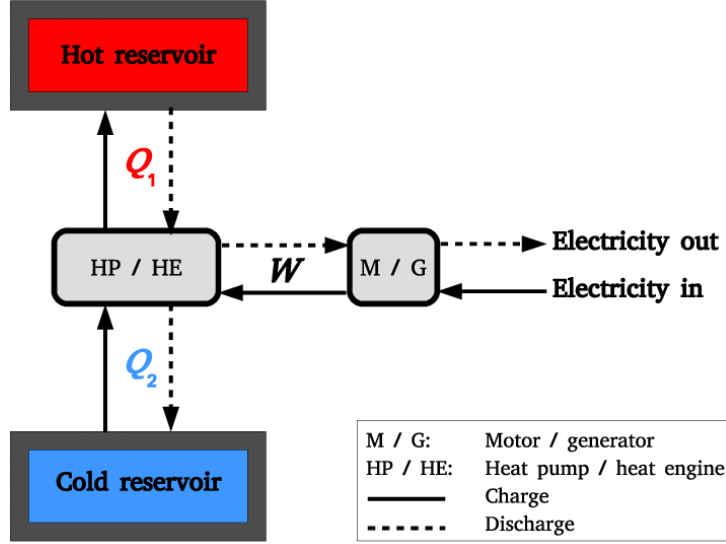


Figure 2.1: Basic scheme of a PTES system acting as a heat pump during charge (solid line) and as a heat engine during discharge (dashed line) [18].

Therefore, the basic configuration of a PTES system consists of the coupling of two main parts: a working circuit, also called power cycle, which represents the working body of the heat engine and heat pump cycles; and a thermal energy storage system, which represents the high-temperature and low-temperature thermal reservoirs levels, between which the cycles operate.

Considering an ideal system, where compression and expansion processes are isentropic and the heat exchanges with the thermal stores are isothermal, the cycle can be represented by a Carnot-equivalent cycle and the round-trip efficiency is given by the COP of the heat pump multiplied by the efficiency of the heat engine:

$$\begin{aligned}
 RTE_{ideal} &= \frac{\dot{W}_{el,out}}{\dot{W}_{el,in}} = \frac{Q_{HR,charge}}{W_{in}} \frac{W_{out}}{Q_{HR,discharge}} = COP * \eta_{HE} \\
 &= \left( \frac{T_{hot}}{T_{hot} - T_{cold}} \right) \left( \frac{T_{hot} - T_{cold}}{T_{hot}} \right) = 1
 \end{aligned} \tag{2.1}$$

In fact, in the case of reversible transformations, the efficiency of the complete charge and discharge cycle is 100%. This happens because, without considering the irreversibility of heat exchange and work exchange, whatever PTES system is considered, the energy absorbed is equal to the one produced. If an ideal Joule-Brayton cycle is considered for the heat engine and the heat pump, it is easy to see that the power absorbed and produced by the compressor and the expander compensate each other in the charge and discharge phase, making the overall efficiency 100%.

However, this ideal efficiency is not practical, since it implies heat addition and rejection at constant temperatures, and is not consistent with the need to progressively heat or cool a thermal storage mass from a charged temperature back to a discharged

one. In reality, PTES round-trip efficiency is lower than one, because of the irreversible processes used to drive the heat pump and the heat engine, which are compression, expansion, heat transfer processes and also heat leakage losses in the tanks and pressure drop losses.

## 2.2. Matching of heat sources and heat sinks with realistic power cycles

In the design process of a PTES system the choice of which thermodynamic cycle to use is strictly related to that of the thermal storage system. In fact, an important challenge is to match the temperature profiles of the heat exchanges between the thermal storage system and the working fluid, in order to have a high overall efficiency of the system. Two examples of good match between storage medium and working cycle are given on the lower part of Figure 2.2 for sensible heat (left) and latent heat (right) storage. In the sensible heat storage case the medium stores heat at variable temperature and the working fluid exchanges heat varying its temperature, while in the latent heat storage case the medium stores heat at constant temperature and the working fluid undergoes a phase change during the heat exchange, so its temperature is constant. Some mismatches between heat sources and heat sinks lead instead to work losses, even if the cycles are ideal and reversible during charging and discharging.

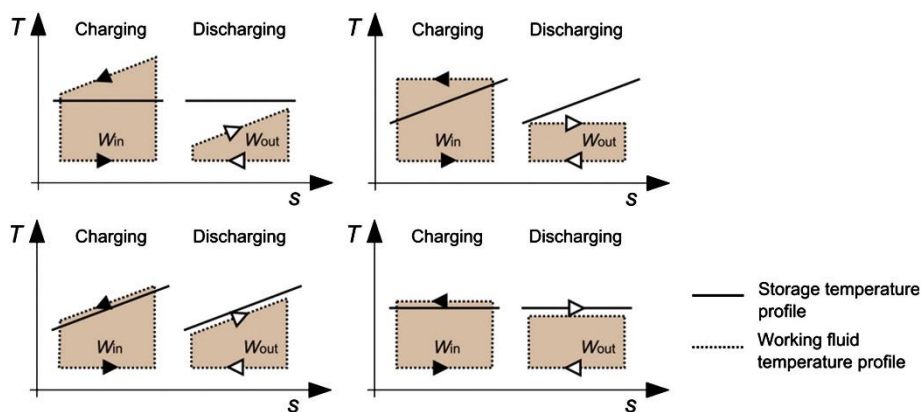


Figure 2.2: Match between the cycle and heat sources/sinks [16].

Although theoretically any thermodynamic cycle can be used in a PTES system, currently the literature shows three main subcategories, based on the type of thermodynamic cycle and consequently on the working fluid adopted:

- Compressed Heat Energy Storage (CHEST), based on water-steam or/and ammonia sub critical Rankine cycle, also called latent PTES;
- PTES based on transcritical CO<sub>2</sub> Rankine cycle;
- PTES based on Brayton cycle with monoatomic or biatomic gases.

In Figure 2.3a the different thermodynamic cycles used for the three concepts are presented, assuming the same working fluid is used. The main trade-off for all types of PTES is between the back-work ratio and the heat storage ratio, according to Abarr et al. [19]. Heat storage ratio is defined as the ratio between the heat delivered to the hot source and the compression work while charging  $Q_{hot, ch}/W_{comp, ch}$  and the back work ratio is defined as the ratio of compression work over expansion work during discharge  $W_{comp, dis}/W_{exp, dis}$ . Comparing the three types of PTES, if we assume to have the same amount of compression work during charge, a low back work ratio means having a higher expansion work and therefore a lower energy stored in the hot reservoir, so in this case the major source of loss are the irreversibilities in the turbomachinery. On the contrary having a high heat storage ratio means having, for the same compression work, a higher heat stored in the hot reservoir and therefore in this case the major source of losses are the heat transfer irreversibilities with the hot reservoir. As it can be seen in Figure 2.3b, the heat storage ratio is inversely proportional to the back work ratio, in fact the Brayton PTES has a high back work ratio and low heat storage ratio, vice versa for the latent PTES, while transcritical PTES lays in the middle of the two.

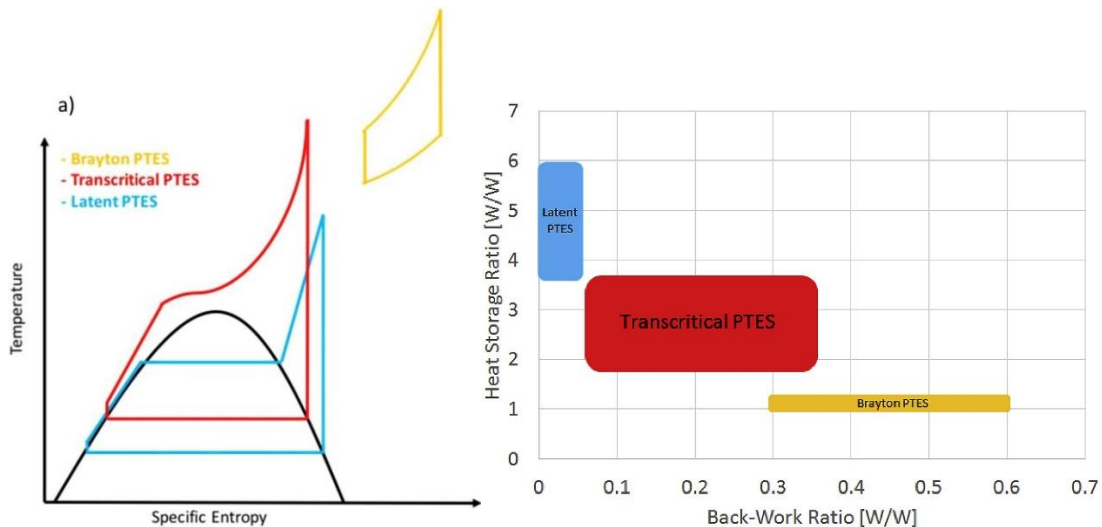


Figure 2.3: Generic T-s diagram for ideal Brayton PTES, Transcritical PTES and Latent PTES cycle (left); Comparison for different PTES types based on ideal cycle analysis. Commonly considered working fluids for PTES (argon, air, water, CO<sub>2</sub> and ammonia) were used to derive these numbers (right).



The present thesis work will focus on the PTES system with Brayton cycle, which is one of the first and most studied cycle configurations.

## 2.3. Description of PTES with Brayton thermodynamic cycle and main components

A PTES system with Brayton cycle in a general configuration, as already mentioned, follows a reversible cycle, which means that the cycle follows an inverse and a direct Brayton cycle during the charge and discharge phase, respectively. Considering an ideal Brayton cycle, the cycle consists of two isentropic compression and expansion processes and two constant pressure heat exchanges.

More in detail, during the charge mode a working fluid, typically a gas, is compressed to a high temperature and pressure condition (1-2) and it gives its heat to the hot reservoir (2-3), while cooling itself down. Then, the gas is expanded to a low temperature and initial pressure condition (3-4), cools the cold store that is at a higher temperature, while increasing its temperature, and it is brought back to the initial condition, before being recompressed.

Upon discharge the fluid direction is reversed, so the working fluid is cooled by passage through the cold store (1-4) and it is compressed until the maximum pressure of the cycle (4-3). Then the nearly ambient temperature fluid discharged from the compressor is heated by passage through the hot store (3-2), prior to expansion in the expander (2-1).

In Figure 2.4 are shown the basic scheme and the T-s diagrams of two ideal PTES systems following a Brayton cycle. During charge the cycle is anti-clockwise and the compressor work is much higher than the expander work, so the mechanical energy absorbed, which is proportional to the area enclosed by the cycle, is transferred into stored heat. During discharge the cycle is clockwise and the area enclosed by the cycle is proportional to the work done.

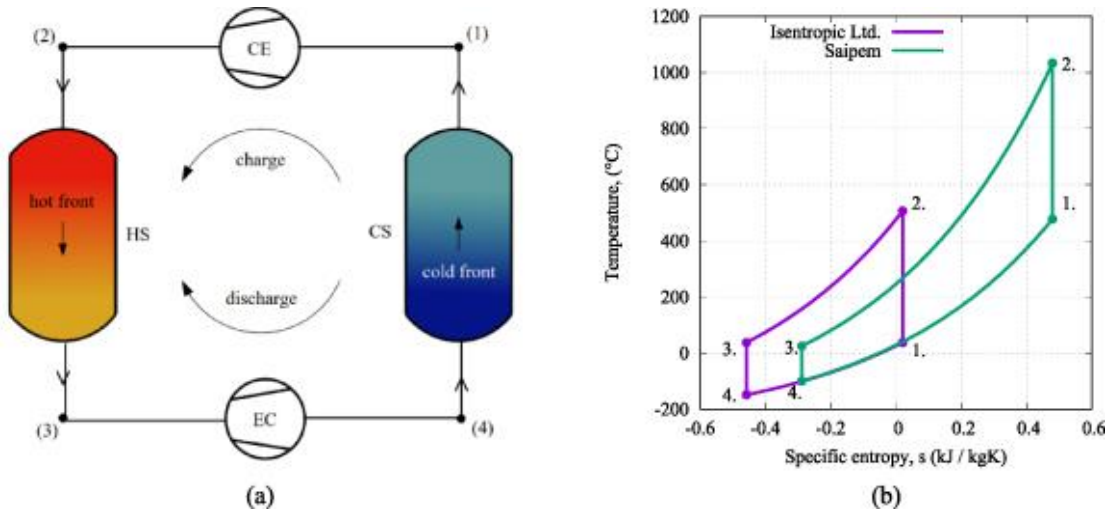


Figure 2.4: (a) Basic scheme of a PTES system using solid thermal storage and (b) T-s diagram of ideal cycles developed by SAIPEM and Isentropic Ltd [20].

The inclusion of the various losses modifies the T-s diagram as shown in Figure 2.5. Entropy increases, during compression and expansion processes, and various pressure losses mean that the charge and discharge cycles are no longer coincident, so as expected the work output falls below the work input during charge. Due to compression and expansion irreversibilities, the temperatures at the inlet of the hot store and cold store tend to increase between each successive cycle. Therefore, to keep them equal to their nominal values, heat must be rejected from the cycle through heat exchangers.

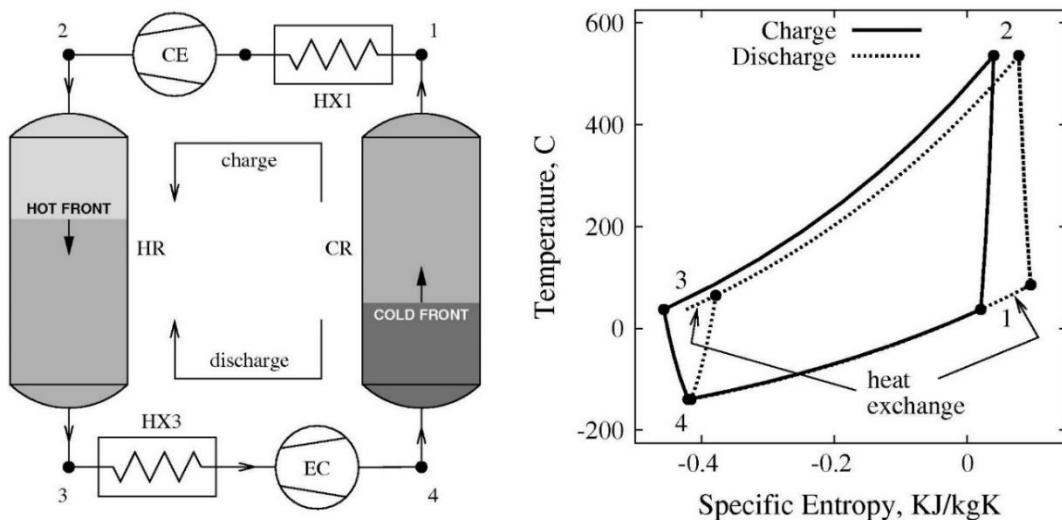


Figure 2.5: Layout of a PTES system and corresponding T-s diagram [21].

Considering the configuration in Figure 2.6 proposed by White et al. [22], if the pressure ratio of the discharge cycle, whose points are denoted by a prime, is the same as that for charging, then the compressor delivery temperature  $T_{3'}$  lies above  $T_3$ , as in Figure 2.6a. Therefore, heat must be rejected via HX2 (see Figure 2.5), such that the hot reservoir can be restored to its initial, discharged state. Likewise, heat must be rejected between states 1 and 1' via HX1 in order to return the cold reservoir to its initial state.

Alternatively, as shown in Figure 2.6b, a lower discharge pressure ratio can be used such that  $T_{3'} = T_3$ . In this case, all the heat is rejected between states 1' and 1 in HX1. In fact, the optimal pressure ratio lies somewhere between these two cases.

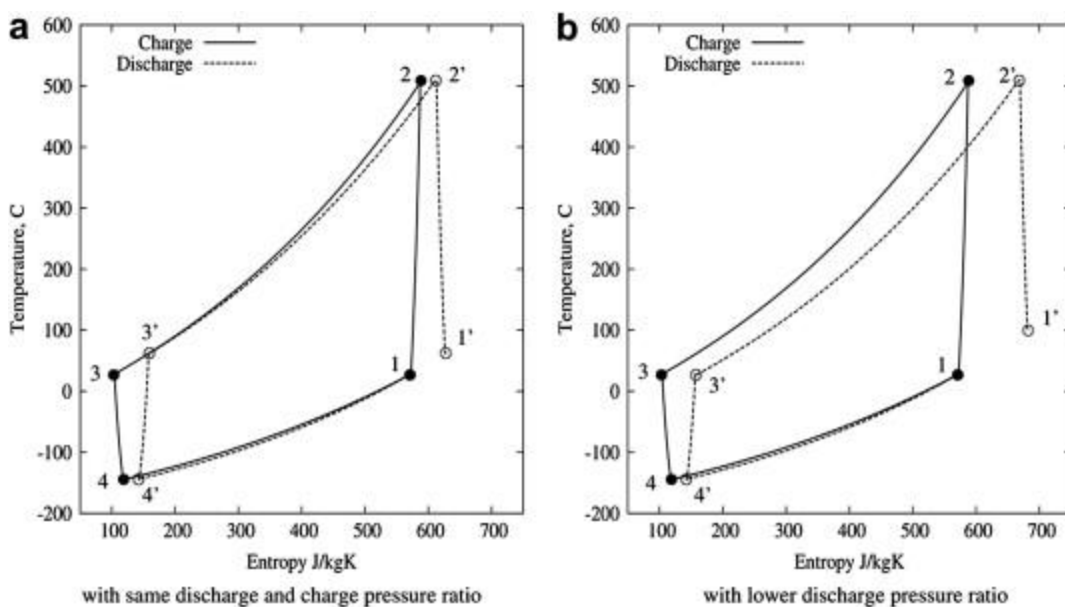


Figure 2.6: T-s diagrams for irreversible PTES cycles [22].

In order to analyze and compare the configurations proposed in the literature it is useful to consider the main components of a Brayton-cycle PTES system. The basic configuration of a PTES system consists of the coupling of a working circuit, also called power cycle or compression-expansion circuit, and a thermal energy storage system.

The first main components of the working circuit are compressors and expanders, represented by C and E respectively in Figure 2.5, and they are usually mechanically coupled and linked to a motor-generator. They can be turbomachinery-based, in which case they are typically organized in two sets, one for charge and one for discharge, or they can be reciprocating devices, where only one set is used for both charge and discharge. Other very important components are heat exchangers, HX1 and HX2, that are required to reject heat from the cycle and maintain near-constant temperatures at the inlets of the two reservoirs, thus achieving steady-state cyclic operation.

The thermal storage system is the other very important part of the PTES system, where the heat produced during the charging cycle is stored. It consists typically of two stores, a hot one and a cold one, which are made by one or more insulated reservoirs, usually tanks or cylindrical vessels. The thermal energy produced can be stored in the form of sensible heat or latent heat.

The materials employed for sensible heat are generally inexpensive and safe ones and can be solid or liquid. Among the liquid materials water is one of the cheapest and most commonly used, but also molten salts, liquid metals and thermal oils are very often employed, depending on their properties and operating temperatures. The most used solid media are concrete, rocks, sand, gravel and ceramic, with various sizes like gravel-sized particles, pebbles or bricks, and they are typically used as filler materials in packed bed (or pebble-bed) configurations of the thermal stores [8].

In the latent heat storage the media are generally called Phase-Change Materials (PCM), because the process is associated with a phase transition. During these transitions, heat can be added or extracted without affecting the material temperature, giving it an advantage over sensible heat technologies. Storage capacities are often higher as well and usually solid-liquid phase change is used. PCMs are further subdivided into organic, inorganic and eutectic materials, each with different properties, and the most used are salts, polymers, gels, paraffin waxes and metal alloys [8].

The coupling of the thermal storage system with the power cycle can be made in two ways, as shown in Figure 2.7:

- Direct storage system (for example thermocline systems), in this case the working fluid, which is the heat carrier, passes directly through the thermal stores, so it is in direct contact with the storage material. As the working fluid passes through the thermal stores, the hot store will always be at, or near to, the compressor delivery pressure, needing a significant pressure vessel to store the hot gravel. It is usually used with solid storage materials and is a cost-effective solution if the medium does not need to be pressurized, avoiding the use of expensive pressure vessels;
- Indirect storage system, in this case the thermal stores have their heat transfer fluid (HTF) that does not pass through the working circuit, so it is usually used with liquid storage materials. The working circuit is essentially the same as the direct system except the near constant pressure heat transfer with the thermal store is done in the decoupling heat exchangers instead of directly with the thermal storage material. The potential advantage is that the thermal stores, in particular the hot store, don't have to be at the elevated pressure of the working circuit and so can operate at near atmospheric pressure.

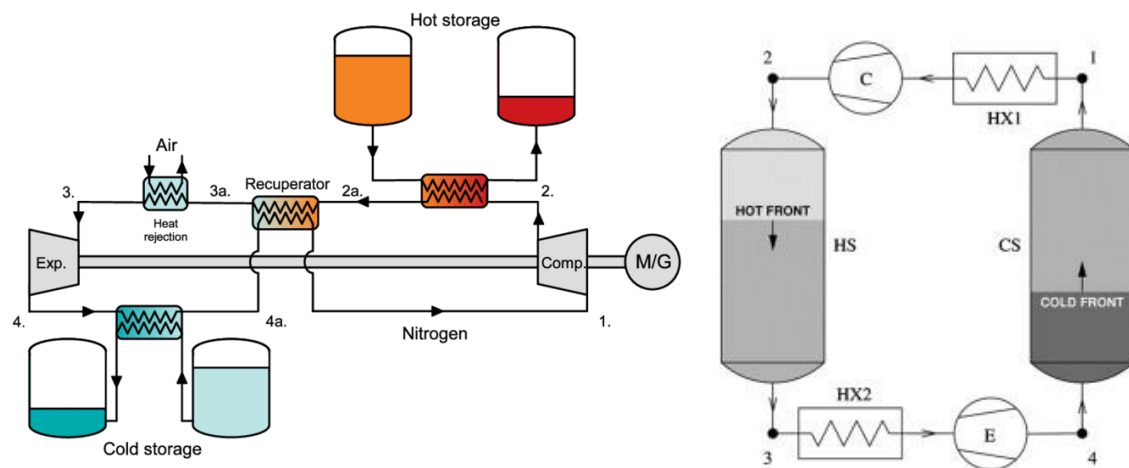


Figure 2.7: (a) Plant layout of an indirect storage recuperated Joule-Brayton PTES system during charge [13]; (b) layout of a direct storage PTES system during charge [22].

The most investigated solutions for solid storage materials are two types of packed bed configurations. The former can be made by insulated vessels, where large blocks of storage material are crossed by channels in which flows the heat transfer fluid, as in the model proposed by Desrues et al. [23]. The latter is made by insulated tanks filled with spheres, pebbles or gravel-sized particles of the storage material, where the heat transfer fluid passes between the particles getting heated or cooled by them.

A liquid storage system uses typically two tanks for the hot and cold storage each, where the hot and cold liquids exchange heat with the working fluid by decoupling counter current heat exchangers.

In order to evaluate the performances of energy storage systems and compare the different configurations adopted (among the same technology), it is useful to consider some rating parameters, which are defined in the following paragraphs.

## 2.4. Rating parameters and notations

It is noted that an assumption in the present work is that conversion processes from electrical energy to mechanical work, and vice versa, have higher efficiencies, are faster and take place in smaller components than those associated with other processes in the technologies of interest, so those associated with mechanical to thermal energy conversion. In this case, overall technical and thermodynamic performance is determined by the latter processes and reference to electrical energy and mechanical work are interchangeable in terms of performance.

A unique attribute of thermo-mechanical energy storage (TMES) systems is that the various flows of heat, cold and electricity facilitate integration with other energy processes. Comparing these advanced systems, however, which involve integration of heat sources and heat sinks, becomes more complicated. When heat is a useful output of the system the requirements regarding the efficiencies and costs of system components are different and, in these cases, the round-trip efficiency becomes less relevant.

### Storage capacity and size definition

The size of an energy storage system (ESS) is usually expressed by the rated net discharge power (in MW) and the storage capacity (in MWh). The capacity of the system is defined as:

$$Capacity = \dot{W}_{el,charge} * t_{charge} \quad (2.2)$$

where  $t_{charge}$  is the charge time and  $\dot{W}_{el,charge}$  is the net electricity power input. Usually, to describe plant sizes, it is used the notation discharge power/storage capacity, in MW/MWh, or discharge power/discharge duration.

### Work Ratio (R)

It is defined as the ratio between compression work to expansion work during charge, or equivalently the ratio of expansion work and compression work during discharge:

$$R = \frac{W_{comp,ch}}{W_{exp,ch}} \quad (2.3)$$

Note that R is always greater than 1 and, for a given net work output, having a high R enables the installation of smaller and more compact machines and the achievement of a higher RTE.

### Energy density ( $\rho_E$ )

Energy density in the field of static energy storage application is defined as the ratio between the nominal electrical energy delivered by the expander during discharge and the total volume of the storage system:

$$\rho_E = \frac{W_{el,discharge}}{\sum V_{storage}} \quad (2.4)$$

where  $W_{el,discharge}$  stands for the net electricity work output during discharge and  $\Sigma V_{storage}$  denotes the total volume of the tanks (reservoirs). The energy density is usually measured in kWh/m<sup>3</sup>.

The energy density is defined also as the available energy stored per unit volume of storage medium, so it can be written as the difference between the stored enthalpies of the two reservoirs:

$$\rho_E = \frac{(H_2 - H_3) - (H_1 - H_4)}{V^H + V^C} \quad (2.5)$$

where H and V are the enthalpy and the volume of the store, and superscripts H and C refer to the hot and cold store respectively. The above equation is written in such a way that it can be applied to systems that may have different storage materials for the hot and cold store.

### Power density ( $\rho_P$ )

The power density is defined here as the power delivered by the system divided by the maximum volumetric flow rate of the working fluid in the cycle:

$$\rho_P = \frac{\dot{W}_{el,discharge}}{\dot{V}_{max}} \quad (2.6)$$

A high power density is preferred because it usually means a lower cost for the turbomachinery, since having a low volumetric flow rate means using more compact devices.

### Round trip efficiency (RTE)

It is defined as the ratio between the energy produced during discharge, so the net work output, and the energy absorbed during charge, so the net work input. It is the most important performance index and represents the overall efficiency of the storage system:

$$RTE = \frac{W_{out}}{W_{in}} = \frac{W_{el,discharge}}{W_{el,charge}} \quad (2.7)$$

Thus, the round-trip efficiency of PTES is limited only by irreversibilities within the cycle. The actual challenge is to find a realistic implementation, so realistic thermodynamic cycles and working fluids, that will result in appropriate pressure ratios with high turbomachine efficiencies, cheap and environmentally friendly thermal storage materials, high heat transfer efficiencies and a suitable external heat source to discharge the overall exergy losses, which cannot be avoided.

The RTE is important also for the definition of the minimum cost of the electricity to be sold in the discharge phase defined as:

$$C_{el,discharge} = \frac{C_{el,charge}}{RTE} \quad (2.8)$$

where  $C_{el}$  is the electricity cost (\$/kWh).

### Levelised Cost of storage (LCOS)

It is described as the total lifetime cost of the investment in an electricity storage technology divided by its cumulative delivered electricity:

$$LCOS = \frac{CAPEX + \sum_{t=1}^{t=n} \frac{A_t}{(1+i)^t}}{\sum_{t=1}^{t=n} \frac{W_{out}}{(1+i)^t}} \quad \left[ \frac{\text{€}}{\text{kWh}} \right] \quad (2.9)$$

$$A_t = OPEX_t + CAPEX_{re,t} + c_{el}W_{in} - R_t \quad (2.10)$$

The capital expenditure (CAPEX) is added to the annual cost  $A_t$  of the storage system at each point of time  $t$  over the lifetime  $n$  of the storage, discounted with the interest rate  $i$ . This sum is divided by the sum of the annual energy outputs  $W_{out}$ , which is also discounted.  $A_t$  is composed of the operation cost  $OPEX_t$ , the reinvestments in storage system components  $CAPEX_{re,t}$  at the time  $t$  as well as the cost of electricity supply, which is determined by the electricity price  $c_{el}$ , multiplied with the annual electricity input  $W_{in}$ . At the end of the storage lifetime a recovery value  $R$  is included.



### 3 Literature review of PTES based on Brayton cycle

Many authors proposed simplified models and developed several expressions, by performing first principles, endo-reversible thermodynamics, or classic cycle analysis, to investigate the behaviour and performance of the PTES system.

A large part of the thermodynamic models in literature proposed sensitivity analyses, showing how the design parameters and the variation of loss factors, operating conditions and geometric parameters influence the performances of the system, in order to develop strategies for optimization.

Many of the models developed analyzed simplified systems in quasi-steady operation. Heat exchangers, compressors and expanders were treated as steady flow devices (in the time-averaged sense), but the equations governing heat transfer within the reservoirs were integrated in time, to track the hot and cold thermal fronts and the transient behaviour of the thermal storages. This is necessary because the stored available energy and the exergetic losses in the reservoirs are dependent upon the time-history of their operation.

The main loss parameters were found to be polytropic (or isentropic) efficiencies of the turbomachinery, pressure losses, heat transfer losses in all the components and heat leakages in the thermal reservoirs.

Before carrying out a literature review, a basic thermodynamic theory is proposed to provide a knowledge of the key dimensionless parameters controlling performance.

### 3.1. Main design parameters and variation of performance with operating conditions

Many thermodynamic models proposed in the literature estimated the influence of main design parameters, such as operating conditions, on the performances of the system to develop strategies for optimisation.

Simple models of ideal Brayton-cycle PTES systems can be developed analytically by using a perfect gas model for the working fluid, and such analysis is worthwhile before developing more detailed models.

Considering a reversible, adiabatic PTES system, as the one in Figure 3.1, White et al. [21] proposed simple expressions for the stored energy that can be converted back to useful work and the power output of the system. The former is calculated as the difference between the stored internal energies of the two reservoirs:

$$E = M_s^h c_s^h (T_2 - T_3) - M_s^c c_s^c (T_1 - T_4) \quad (3.1)$$

Here  $M_s$  is the mass of storage material,  $c_s$  is its average specific heat capacity over the relevant temperature range, and the superscripts h and c refer to the hot and cold reservoirs, respectively.

The power output was given instead by:

$$\dot{W} = \dot{m} c_p [(T_2 - T_1) - (T_3 - T_4)] \quad (3.2)$$

where  $\dot{m}$  is the mass flow rate of the working fluid.

Many authors considered convenient to use a polytropic process to describe the compression and expansion processes, since it does not depend on the compression ratio. Therefore, with reference to the T-s diagram in Figure 3.1, the temperature difference across the turbomachines can be described by the isentropic compressor, or expander, temperature ratio  $\tau = T_2/T_1 = T_3/T_4$ , which is linked to the pressure ratio by the expression:

$$\tau = \beta^{(\gamma-1)/\gamma} \quad (3.3)$$

where  $\beta$  is the pressure ratio and  $\gamma$  is the isentropic index of the gas, which is the ratio of  $c_p$  over  $c_v$  of the gas. In order to describe the real process and to take account of the turbomachine irreversibilities, it can be considered a polytropic efficiency  $\eta$ , so that the compression and expansion can be written as:

$$\left( \frac{T_{out}}{T_{in}} \right)_{comp} = \tau^{1/\eta} \quad (3.4)$$

$$\left(\frac{T_{out}}{T_{in}}\right)_{exp} = \tau^{-\eta} \quad (3.5)$$

Many studies show that, for a given technology, the capital cost per unit energy storage capacity and per unit power capacity will depend inversely on the energy storage density  $\rho_E$  and power density  $\rho_P$ , respectively. These are thus key performance parameters in the design of any storage method.

Their dependence on the temperatures of the cycle are given in simplified expressions, developed by White et al. [22], for fully reversible PTES systems with the same solid packing material in both reservoirs, as shown in Figure 3.1:

$$\rho_E = 1/2 \rho_s c_s [(T_2 - T_1) - (T_3 - T_4)] = 1/2 \rho_s c_s T_1 (\tau - 1) \left(1 - \frac{\theta}{\tau}\right) \quad (3.6)$$

$$\rho_P = \rho_{g1} c_{pg} [(T_2 - T_1) - (T_3 - T_4)] = \frac{\gamma}{\gamma - 1} p_1 (\tau - 1) \left(1 - \frac{\theta}{\tau}\right) \quad (3.7)$$

Where  $\rho_s$  and  $\rho_{g1}$  are the storage medium and gas density respectively (at state 1 for the latter),  $c_s$  and  $c_{pg}$  are the corresponding specific heat capacities (isobaric for the gas) and  $\theta = T_3/T_1$  is the ratio between the hot and cold reservoir temperatures when discharged.

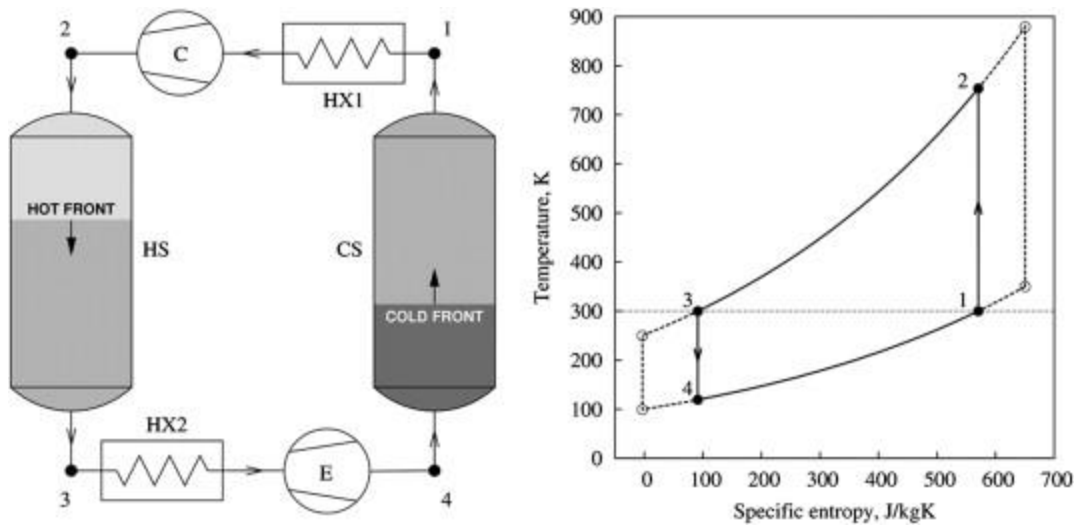


Figure 3.1: Layout of a PTES system and T-s diagram of the ideal cycle during charge [22].

The following may be deduced from these expressions:

- Both the energy and power density are monotonically increasing functions of the temperature ratio  $\tau$ , so also of the pressure ratio;

- For a given pressure ratio (or  $\tau$ ),  $Q_E$  and  $Q_P$  are both increased by reducing  $T_3$  or increasing  $T_1$ . This is also shown by the dashed line in the T-s diagram of Figure 3.1, which encloses a larger area;
- The power density may also be increased by raising the overall system pressure. The factor  $\gamma/(\gamma - 1)$  also has a significant influence and takes the value 5/2 for monatomic and 7/2 for diatomic gases.

The overall efficiency of the system is commonly measured using the roundtrip efficiency  $\eta_{RT}$ .

White et al. [22] developed an approximate expression for the efficiency, based on the irreversibility in the compressors and expanders and assuming ideal heat transfer in the thermal reservoirs. By scaling the ideal compression work by  $1/\eta_s$  and the ideal expansion work by  $\eta_s$ , where  $\eta_s$  is as an average isentropic efficiency, they obtained:

$$\eta_{RT,WPM} = \frac{\eta_s(T_2 - T_1) - (T_3 - T_4)/\eta_s}{(T_2 - T_1)/\eta_s - \eta_s(T_3 - T_4)} = \frac{R\eta_s^2 - 1}{R - \eta_s^2} \quad (3.8)$$

where  $R$  is the work ratio. In fact, for an ideal Brayton cycle, noting that  $T_2/T_1 = T_3/T_4$  under the assumption of perfect gas, the work ratio can be expressed also as:

$$R = \frac{W_{comp}^{ch}}{W_{exp}^{ch}} = \frac{(T_2 - T_1)}{(T_3 - T_4)} = \frac{T_1}{T_4} = \frac{T_2}{T_3} = \frac{\tau}{\theta} \quad (3.9)$$

Thess [15] derived an alternative expression, using an endo-reversible approach, which assumes that irreversibilities are the result of heat transfer between the thermal reservoirs and the thermodynamic cycles that interact with them. Thess's expression has been widely cited, however Guo et al. [24] noted that a mistake had been made and found the correct expression to be:

$$\eta_{RT,GCCZ} = \frac{(T_2/T_4)^{1/2} - 1/2}{(T_2/T_4)^{1/2} + 1/2} = \frac{\tau\theta^{1/2} - 1/2}{\tau\theta^{1/2} + 1/2} \quad (3.10)$$

They determined the optimally operating region of round-trip efficiency and power output of the system using some controlling parameters, for example the maximum temperature of the cycle  $T_2$  and the temperature ratio. This analysis involved maximizing the power output of the heat engine, which is an unrealistic assumption as PTES is unlikely to be operated in this way. The heat pump is not treated in an equivalent way since the heat pump power cannot be optimised.

Laughlin [25] also derived an expression for the roundtrip efficiency that considered the performance of compressors and expanders using the polytropic efficiency  $\eta_p$ .

$$\eta_{RT,L} = 1 - \frac{T_0}{T_1 - T_4} \left( \frac{1 - \eta_p^2}{\eta_p} \right) \frac{\tau \ln \tau}{\tau - 1} = 1 - \left( \frac{1 - \eta_p^2}{\eta_p} \right) \frac{\tau \ln \tau}{(\tau - 1)(\tau\theta - 1)} \quad (3.11)$$

These three correlations are plotted in Figure 3.2 for two values of  $\theta$ , which include the likely range of values of this parameter, and are also shown some data points developed in the literature using more detailed models.

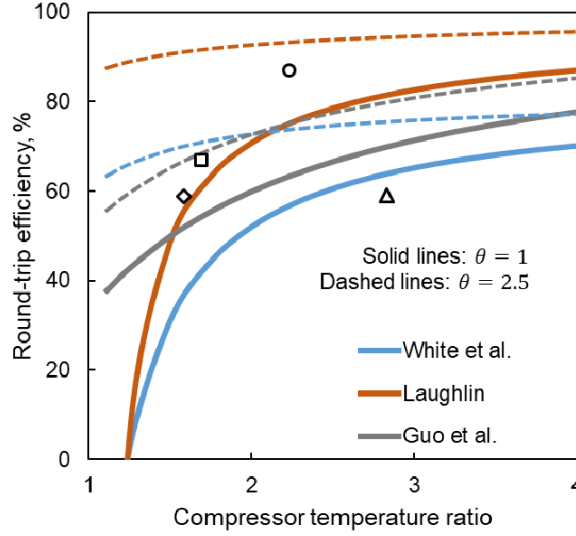


Figure 3.2: Roundtrip efficiency correlations of Brayton-cycle PTES with  $\eta_i = 90\%$ . The points represent data from literature.  $\square$ : SAIPEM design with  $\eta_p = 90\%$  (Desrues et al., 2010).  $\Delta$ : Isentropic design with  $\eta_p = 90\%$  (McTigue, White and Markides, 2015).  $\odot$ : Isentropic design with  $\eta_p = 99\%$  (McTigue, White and Markides, 2015).  $\diamond$ : Malta design with  $\eta_p = 90\%$  (Olympios et al., 2021).  $\theta = T1/T3$  [13].

Similarly to the work ratio, the heat-to-work ratio provides an assessment of the total heat processed by the cycle for a given net work input:

$$\tilde{Q} = \frac{\sum |Q|}{W_{in}^{net}} = \eta_s \frac{\tau/\theta - 1}{\tau/\theta - \eta_s^2} * \frac{\tau + 1}{\tau - 1} \quad (3.12)$$

Large heat-to-work ratios are typically undesirable because, for a given net work input, a large quantity of heat must be transferred, thus heat transfer irreversibilities have a large impact on the cycle performance and larger heat exchangers will be required.

In Figure 3.3 is illustrated the impact of the compressor temperature ratio  $\tau$  and  $\theta$  on the work ratio and heat-to-work ratio for cycles with an isentropic efficiency of 90%.

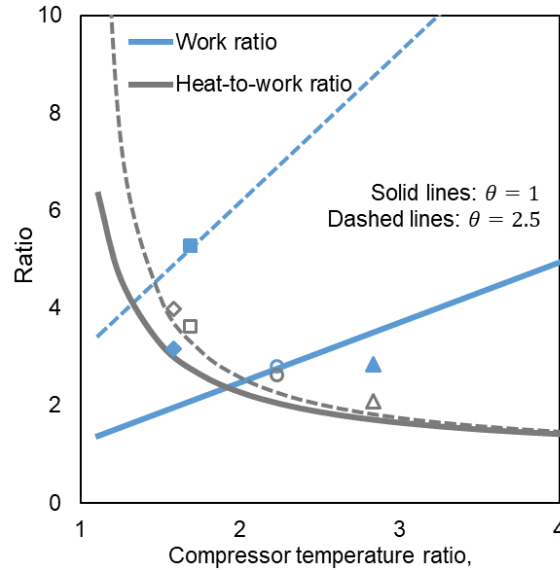


Figure 3.3: The work ratio and heat-to-work ratio can inform the design of PTES systems for  $\eta_i = 90\%$ . The points represent data from the literature. Blue points are work ratios and grey points are heat-to-work ratios.  $\square$ : SAIPEM design (Desrues et al., 2010).  $\triangle$ : Isentropic design with  $\eta_p = 90\%$  (McTigue, White and Markides, 2015).  $\odot$ : Isentropic design with  $\eta_p = 99\%$  (McTigue, White and Markides, 2015).  $\diamond$  Malta design with  $\eta_p = 90\%$  (Olympios et al., 2021).  $\theta = T1/T3$  [13].

This analysis shows that the round-trip efficiency and the energy storage and power densities increase monotonically with the temperature ratio, which depends on the pressure ratio and the isentropic index of the gas. It is also found that the round-trip efficiency and the storage density are particularly dependent on the compression and expansion polytropic efficiency, especially at low temperature (and hence pressure) ratios, and for given compression and expansion efficiencies they increase as  $R$  increases.

As noted by Farres-Antunez [26], the net work input to the charging phase may be written as  $W_{\text{net}} = (R - 1)W_{\text{comp}}$ , so it can be seen that low work ratios mean large machines are required to achieve a given net work input. In addition, low values imply that a large quantity of work is ‘processed’ for a given work input. Thus, cycles with high work ratios are less sensitive to compression and expansion losses, because losses have a smaller effect on the net work input.

High work ratios can be obtained by increasing the pressure ratio, but also decreasing the ratio  $\theta$ , so decreasing the hot reservoir discharged temperature  $T3$  or increasing the cold reservoir discharged temperature  $T1$ . These solutions are both consistent with improving the energy and power densities and also the roundtrip efficiency. They also reduce the effect of compression and expansion losses, but the heat-to-work ratio increases, meaning that heat exchanger performance becomes more important, because larger heat exchangers are required.

White et al. [21] also underlined that reducing  $\theta$  improves the round-trip efficiency especially for turbomachinery-based systems. Such benefits would not be realised however if the maximum and minimum temperatures within the cycle were to be constrained.

If  $T_1$  is fixed, increasing  $\tau$  means increasing the maximum temperature of the cycle and decreasing  $\theta$  results in the decrease of the minimum temperature of the cycle. Therefore, the main cycle constraints are represented by the maximum and minimum temperature  $T_2$  and  $T_4$ . The work ratio can be rearranged and written as a function of  $\tau$ ,  $T_2$  and  $T_4$  as:

$$R = \frac{T_2}{\tau * T_4} \quad (3.13)$$

Once the maximum and minimum temperature are fixed the R ratio increases as  $\tau$  decreases, so when  $T_1$  increases.

In the direct storage systems however, high temperature ratios imply high pressure ratios, which lead to high storage costs, since hot reservoir needs to be pressurised and requires high cost materials. For this reason a monoatomic gas such as argon is proposed as the working fluid, rather than air, since the same value of  $\tau$  can be achieved at a lower pressure ratio, due to argon's higher isentropic index.

Different technologies and materials may be used at each stage of the process, so that a variety of concepts have been proposed. The rest of this section discusses trade-offs between Joule–Brayton PTES design decisions.

## 3.2. Historical background

The first example of a PTES layout based on an open (power) cycle was proposed and patented in 1979 by Weissenbach of Messerschmitt-Bölkow-Blohm (MBB) [27].

In Weissenbach's system atmospheric air was used as the working fluid and the cold store consisted of a regenerator at atmospheric temperature and pressure. The hot store was specified to be around 800–900°C, with thermal energy stored in ceramic balls contained in steel tubes. Little further information is available to the knowledge of the author, so it is unclear what temperatures  $T_2$  and  $T_3$  were and therefore what the pressure ratio was, but Weissenbach anticipated efficiencies in the region of 65–75%.

In recent years two independent patents seem to have emerged almost simultaneously in 2008-2009 for similar schemes, which are referred to here as the Saipem approach [28] and the Isentropic approach [29], after the companies that filed the patents.

The Saipem scheme, patented by Ruer [28] in 2008, was the first to suggest using argon as the working fluid. The system was based on a closed cycle, where the thermal stores consisted of porous refractory material, or clay with a high content of magnesia, alumina and lime. This material was formed into bricks and perforated with cylindrical holes for the working fluid to pass through. Compression and expansion were undertaken with turbomachinery, meaning that two pairs of compressor and expander are required, one for charging and one for discharging. The layout of Ruer PTES system is shown in Figure 3.4.

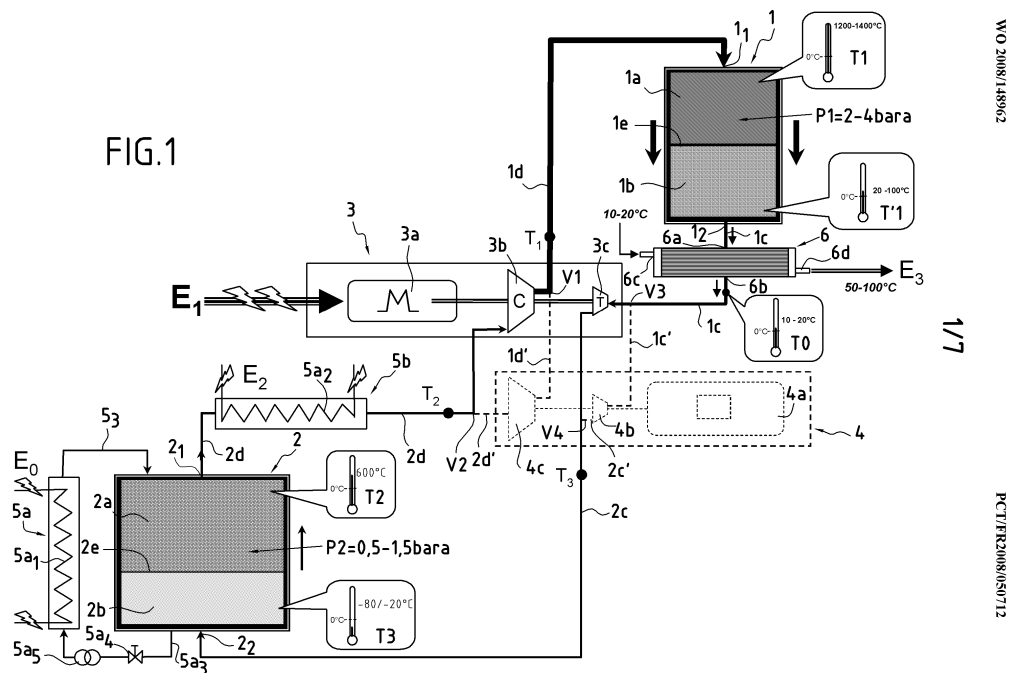


Figure 3.4: Layout of Ruer PTES system.

With reference to the T-s diagram for a typical Saipem scheme, shown in Figure 3.5, the original design uses a low pressure ratio of around 4, but achieves a high work ratio by increasing the value of T1 to around 480°C and fixing T3 to ambient temperature. The low pressure ratio should reduce the cost of the system, although the use of four turbomachines would be expensive.



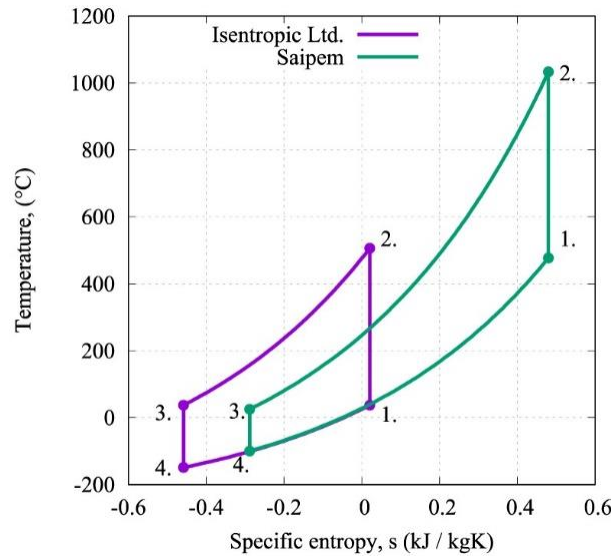


Figure 3.5: T-s diagrams for Joule-Brayton PTES systems proposed by Isentropic and Saipem.

The Isentropic system, patented by J. MacNaghten and J. S. Howes [29] in 2009, also utilises a closed cycle with argon as the working fluid, but compression and expansion, unlike the Saipem scheme, are achieved with reciprocating piston engines. These devices, with a prototype patented by the authors [30], can work both as a compressor and as an expander by changing the valve timings. Consequently, only two devices are required: one on the 'hot' side, to carry out compression during charge and expansion during discharge; and another on the 'cold' side, to expand during charge and compress during discharge. Isentropic efficiencies of reciprocating devices may be in the range of 75-85%, but much of the loss is due to valve pressure losses.

Isentropic Ltd. aimed to reduce these losses significantly, by developing bespoke reciprocating devices with a new valve system, and (perhaps optimistically) quoted isentropic efficiencies of 95-99% [14].

The original patent suggested that the thermal stores would consist of particles or fibres randomly packed to form a gas-permeable structure and allow the gas to flow through. These particles may have a low thermal inertia and would be metallic or possibly a mineral, ceramic or even gravel.

A scheme of this PTES system is represented in Figure 3.6. With reference to the T-s diagram shown in Figure 3.5, the original design uses a pressure ratio of around 12, with a ratio of the reservoirs outlet temperatures  $T_3/T_1 = 1$ . Further details show it has a lower work ratio than the Saipem scheme. Achieving high round-trip efficiencies therefore depends heavily upon developing reciprocating devices with high isentropic efficiencies.

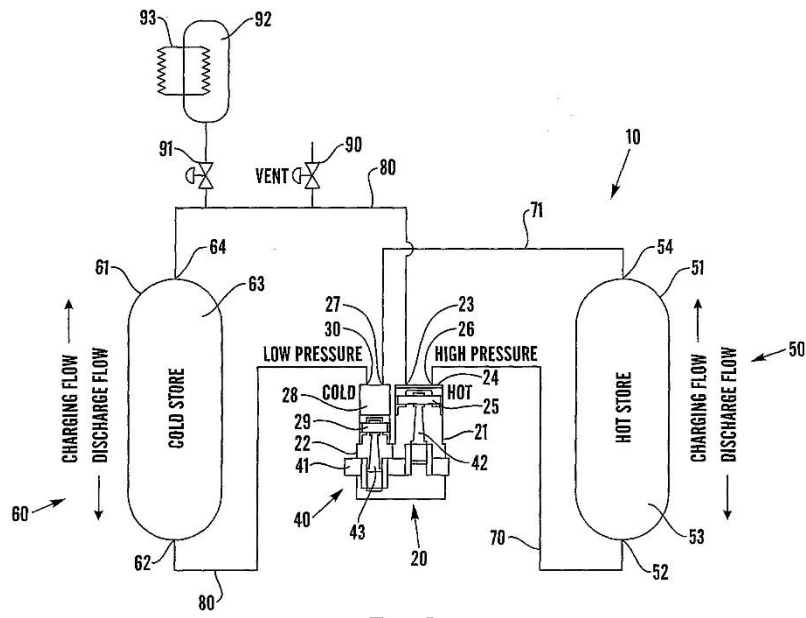


Fig. 1

Figure 3.6: Layout of the PTES system proposed by MacNaghten and Howes [29].

More recently, a Google X spin-out company known as Malta Inc. began the development of a regenerated closed cycle [31], [32], as illustrated in Figure 3.7, with the aim to use commercial or near-to-commercial technologies for each component. Thus, air-based turbomachinery is used for the compression and expansion, keeping temperatures below 600 °C to reduce steel costs. Molten salts are used for the hot storage, while the cold storage uses a coolant such as a water-glycol mixture or isopropane.

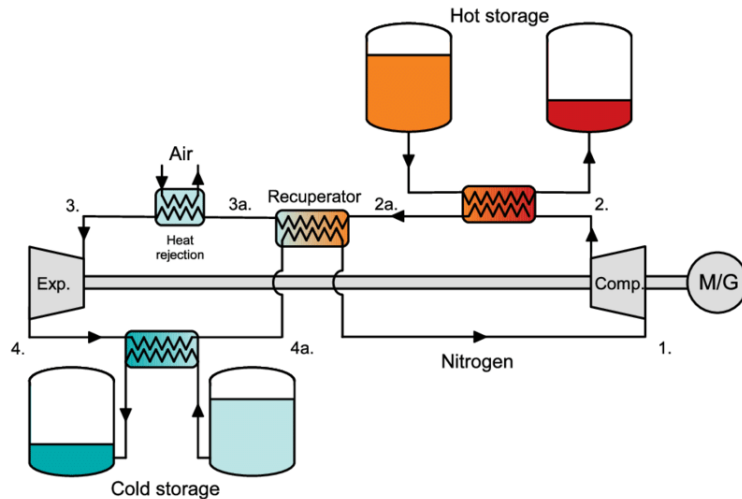


Figure 3.7: Layout of the PTES system proposed by Laughlin et al. [31].

Table 3.1: Operating conditions for Joule-Brayton based PTES systems suggested by patents.

	<b>Saipem</b>	<b>Isentropic Ltd</b>	<b>Malta Inc</b>
Storage type and materials	Concrete bricks	Packed bed of mineral pebbles	HR: molten salts CR: glycol
Polytropic efficiency	0,90	0,90	0,91(c)/0,94(e)
Pressure ratio	2-4	12	~3
T <sub>1</sub> (°C)	400 – 1000	45	220
T <sub>2</sub> (°C)	1000 – 1500	500	550
T <sub>3</sub> (°C)	10 – 50	45	25
T <sub>4</sub> (°C)	-80 – -20	-166	-28
Work ratio, R	~4	2,4	-
Efficiency, RTE (%)	>60	~60	<72

### 3.3. Cycle configuration

The power cycle considered in literature for a Brayton PTES system, as already mentioned, can be open or closed.

Closed-cycle systems, as the ones proposed by Isentropic Ltd, Saipem and Malta Inc, operate as a heat pump and heat engine, transferring heat between a hot and a cold reservoir. The storages must be well insulated, to minimise thermal losses and heat leakages, but allow the cycle to be pressurised. This solution acts to increase the power density of the compression and expansion machinery, reducing their size, for a given power rating, and in theory also the cost of these components. On the other hand, high pressures require strong insulation and sealing to minimise pressure losses, so the cost of the system can be increased, also because of the need of heat rejection components.

Although most of the concepts use a closed cycle, an open-cycle system, as the one proposed by Weissenbach [27], has the main advantage of drawing, and releasing, air

directly from the environment. Moreover, the environment is used as the low-temperature heat storage unit, thereby circumventing the need for heat rejection components, reducing capital and installation costs.

Open-cycle designs however, cannot be pressurised, which means that larger, more expensive, compression and expansion devices are required. In addition, they provide less flexibility in terms of cycle optimisation and working fluid choice. In fact, in closed cycles systems the temperatures and pressures at each point can be optimised to achieve the best possible roundtrip efficiency and work ratio.

These are some of the main reasons why closed cycle solutions are more investigated, however the cost of some components, such as heat exchangers, valves and seals, can also be affected by higher pressures.

### 3.4. Working fluid selection

While an open-cycle PTES systems use atmospheric air as the working fluid, a closed-cycle PTES system can adopt a large variety of options. The selection of the working fluid used in the power cycle must satisfy some main requirements, such as chemical inertness, cheapness, and environmental friendliness. Considering the physical properties, the gases need to be extremely stable at high temperatures and far from liquefaction or solidification phase transitions.

Many authors have investigated the use of different working fluids and their influence on the system performances. Following the analysis conducted by Farres-Antunez [26] and Albert et al. [33], some of them have been selected as the most appropriate and are reported in Table 3.2.

Table 3.2: Main properties of selected working fluid options.  $T_{crit}$  and  $p_{crit}$  represent the critical temperature and pressure, respectively; and MM the molar mass of the fluid.

Working fluid	$T_{crit}$ [K]	$p_{crit}$ [bar]	MM [kg/kmol]	$C_p$ [J/(kgK)]	$\gamma$ [-]
Air	133	38	29	1005	1,4
Argon (Ar)	151	49	39	520	1,667
Helium (He)	5	2	4	5192,6	1,667
Hydrogen (H2)	33	13	2	14307	1,405

Nitrogen (N <sub>2</sub> )	126	34	28	1039	1,4
Oxygen (O <sub>2</sub> )	155	51	32	918	1,395
Neon (Ne)	44	28	20	1029,9	1,667

It can be noticed that all considered fluids have a critical temperature significantly lower than the typical ambient temperature.

In the case of direct storage systems, the packed-bed vessels and the insulated tanks are pressurised. In this case, working fluids with a high isentropic index  $\gamma$ , also known as ratio of specific heats, can achieve the required temperature ratios with lower pressure ratios, which allows to minimize the storage size required and the sealing problem of the storages. For these systems, argon and helium achieve higher energy densities and roundtrip efficiencies than nitrogen and air. However, the choice of storage material for the hot and cold packed beds largely affects the energy density of the system, so methods for the simultaneous optimisation of storage materials and working fluids should be employed.

Argon was preferred by a large part of the packed bed systems investigated, for example the model proposed by Howes [14], Davenne et al. [34], the ones based on the Saipem scheme [23], [35] and the Isentropic scheme [21], [22], [36], [37]. Benato [38] considered air as the working fluid, because of good heat transfer properties and cheapness, while a comparison between argon and air was made by some authors, like Salomone-González et al. [39] and Chen et al. [40], which showed similar performances for the two fluids. Another study by Zhang et al. [41] used helium to compare the performances of a direct storage and an indirect storage configuration, adopting nitrogen as the working fluid in TES circuit in the indirect storage case.

Moreover, a study by Wang et al. [42] showed that at a certain charge pressure ratio, a higher efficiency but a lower energy storage density is obtained with a monoatomic gas than those with a diatomic gas. The round-trip efficiency and energy storage density of the diatomic gas under a large pressure ratio behave similarly to those of the monoatomic gas at small pressure ratios. However, the physical properties, such as density, viscosity, and heat transfer performance of the gasses, have impact on the heat transfer and the pressure loss in components, such as storage beds and HXs.

In the case of liquid-tank storage, the tanks do not have to be pressurised, being decoupled from the working circuit. It is demonstrated for example in the work of Farres-Antunez [26] that, under these conditions, a working fluid is advantageous when it has a high specific heat capacity  $c_p$ , so when it is a diatomic gas instead of a monoatomic gas. This gives advantage to helium and hydrogen. Both gases, however, have a small molecular mass and involve significant leakage issues. Furthermore,

unlike the other options, hydrogen is highly flammable and requires careful handling, so helium have been considered in few studies, like the ones by Zhang et al. [43] and Wang et al. [44]. Nitrogen instead has the advantage that it can be used with commercially available air-based turbomachines, as in the Malta Inc design [25], and it has been considered in the study by Wang et al. [45], McTigue et al. [46] and Yang et al. [47].

Frate et al. [48] compared from the techno-economic point of view a liquid-based and a solid-based configuration, considering air, argon and nitrogen. The most suitable operating fluid was air for both technologies, simplifying the plant management and achieving cost reductions between 1% and 7% compared to argon, according to the considered configuration.

### 3.5. Thermal storage system configurations

Many of the Brayton-cycle PTES designs proposed rely on sensible heat storage materials, either solids or liquids, because they are the most suitable to be integrated with the variable temperature profile of the working fluid in the cycle during the heat exchange.

Until now, the use of latent heat storage has been marginally explored within the context of Brayton-cycle PTES [33], because it is associated with the disadvantages of preventing independent sizing of the energy and power capacity of the system [26], as well as design complexity problems. However, latent heat storage has other advantages, for example more stabilised temperatures and increased heat transfer rates, and it is gaining increasing attention and maturity in the recent years, leading to its investigation in other types of PTES systems.

As already mentioned, the working circuit can be coupled with the TES system by means of a direct storage system or an indirect storage system.

Solid storage materials are mostly used in packed bed or insulated vessel configurations. In fact, the first configurations considered in literature for the thermal storage reservoirs were packed bed systems and large reservoirs where gas-solid heat exchange takes place.

Using a liquid storage medium, instead, requires indirect heat transfer between the power cycle and the storage fluid via decoupling heat exchangers. Being the working circuit and the TES circuit decoupled, the liquid may not have to be pressurized, the cost of the storage tanks can be reduced. Liquids tend to have more limited operating temperature ranges and thus tend to be implemented in recuperated cycles. They also

have higher capital costs and may degrade over time, however some relevant fluids, for example molten salts, have been widely deployed in CSP plants, so the system can benefit from this operational experience and cost reductions.

The main desired properties of heat storage materials may be classified into three categories: thermo-physical, so for example specific heat capacity, thermal conductivity, density and working temperature range; economic, so cost of ownership and operating costs; and safety-related, so flammability or toxicity.

The next section provides a description of possible storage materials and several challenges associated with the choice of storage method.

### 3.5.1. Solid storage systems

Solid storage is particularly well suited for packed beds, where there are gas-phase heat source or heat sink streams. Packed-bed thermal reservoirs typically contain a solid storage material composed of spheres, irregularly shaped pebbles or gravel, or have some other internal structure, such as a concrete structure, through which the heat transfer fluid passes. The packing material is encased in one or more layers of thermal insulation and a steel containment vessel, which may be pressurized for the hot store in PTES. These PTES pressure vessels are usually cylindrical, with closed ends, but other shapes have also been investigated.

A schematic diagram of a packed bed hot store is shown in Figure 3.8. Here the packing material has a length  $L$  and a diameter  $D$ , although the store itself will be larger than this due to the insulation and steel containment.

The pebbles form a porous medium, in which porosity and permeability depend on the shape and size of the particles. These have a diameter of  $d_p$ , which can vary from few millimeters to some centimeters, and occupy a fraction of the store given by  $(1-\epsilon)V$ , where  $\epsilon$  is known as the void fraction or porosity. Some examples of these factors used in literature are given in Table 3.3.

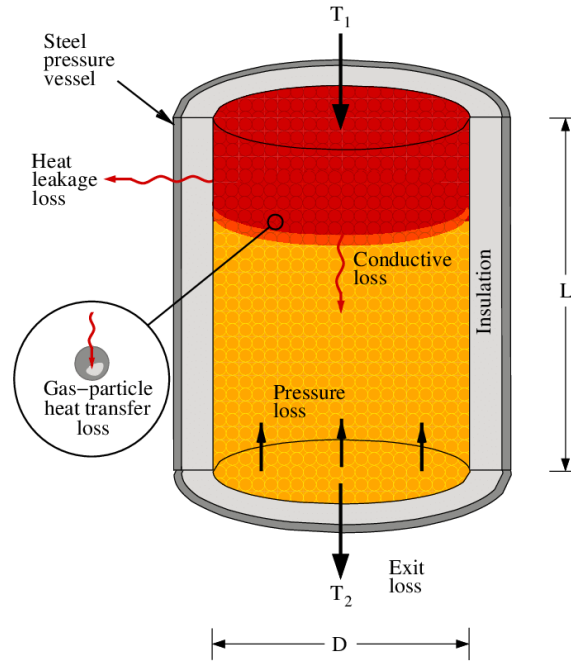


Figure 3.8: Schematic layout of a packed bed. The hot thermal reservoir is orientated vertically during charge. Gas enters at  $T_1$  and exits at  $T_2$ .

Table 3.3: Types and characteristics of packed bed storage systems used in literature.

Authors	Storage material	Material shape and size	Reservoirs dimensions	Void fraction	Others
Desrués et al. [23]	Concrete	Bricks	$V_{\text{total}} = 21622 \text{ m}^3$	0,44	-
Howes [14]	Particulated granite	-	-	-	-
McTigue et al. [21]	Magnetite ( $\text{Fe}_3\text{O}_4$ )	Spherical pebbles, $d_p = 2\text{cm}$	HR: $D = L = 4,5 \text{ m}$ , $V = 71 \text{ m}^3$ CR: $D = L = 5,3 \text{ m}$ , $V = 117 \text{ m}^3$	0,35	-
Ni and Caram [35]	Basalt	Spherical stones, $d_p = 8 \text{ cm}$	HR/CR: $D = 3 \text{ m}$ , $L = 32 \text{ m}$	0,4	-
Benato [38]	Aluminum oxide ( $\text{Al}_2\text{O}_3$ )	Spheres, $d_p = 15 \text{ cm}$	HR/CR: $L = 10 \text{ m}$ , $V = 150 \text{ m}^3$	0,4	-
Wang et al. [45]	Granite	Pebbles, $d_p = 0,9 \text{ cm}$	CR: $D = 34,5 \text{ cm}$ , $L = 1,5 \text{ m}$	-	-



Wang et al. [36]	Basalt	Particles	HR: V = 460 m <sup>3</sup> CR: V = 740 m <sup>3</sup>	-	-
Davenne et al. [34]	Quartz gravel	Pebbles, d <sub>p</sub> = 0,04 - 1 cm	HR: V = 30000 m <sup>3</sup> CR: V = 60000 m <sup>3</sup>	0,5	Comparison of coupled and decoupled (N <sub>2</sub> as TES fluid)
Wang et al. [44]	Basalt	Pebbles, d <sub>p</sub> = 3 cm	HR: V = 920 m <sup>3</sup> CR: V = 1480 m <sup>3</sup>	0,4	HR/CR: 3, 5, 7
Zhang et al. [41]	Basalt	Pebbles, d <sub>p</sub> = 3 cm	HR: D = 7,7 m, CR: D = 9,72 m L/D = 1,5	0,4	-
Ge et al. [37]	PCM	PCM capsules, d <sub>p</sub> = 2 cm	HR: D = 3,88 m, L = 6 m, V = 71,1 m <sup>3</sup> CR: D = 2,61 m, L = 6 m, V = 32,1 m <sup>3</sup>	0,4	-
Albert et al. [33]	SH: magnetite LH: PCM	SH: pebbles LH: encapsulated particles, d <sub>p</sub> = 2 cm	HR: 21 m <sup>3</sup> CR: 46 m <sup>3</sup>	0,5	-

The first Joule–Brayton cycles proposed in literature used solid materials. In fact, Weissenbach’s system used ceramic balls in steel tubes; SAIPEM’s design used a concrete thermocline system and Isentropic Ltd used packed beds of pebbles.

The forced convective heat transfer between fluid and storage materials in packed-beds is complex, so the system design requires careful optimization. Several models have been explored to capture the transient behaviour of packed-bed stores, including one-dimensional and two-dimensional heat transfer approaches.

Desrues et al. [23] were among the first to develop a model for the packed bed with a finite volume scheme where, using a simplified geometry and taking into account turbomachinery efficiency, they analysed the related losses due to the moving thermal front.

The thermal front, often called thermocline, is a moving thermal gradient along the bed length, which results from the transfer of heat through convection from the gas to the solid. The specific heat capacity of the solid is a function of its temperature, and thus changes along the length of the store, significantly affecting the shape of the

thermal front and the thermal losses [21], [49]. Considering this phenomenon, a large part of the configurations proposed assumed that the working fluid enters at the top of HR and exits at the bottom, while for the CR it enters at the bottom and exits at the top, in order to prevent buoyancy-driven instabilities of the thermal fronts. In fact, a study by McTigue et al. [50] showed that the shape of the thermal front is affected by the chosen design and experiences changes throughout the charging and discharging operations. This is important because changes in the shape of the thermal front determine a variation of the temperature of the fluid exiting the store. This in turn disturbs the smooth operation of the cycle and doesn't allow the rest of the system, including the compressors and expanders, to be optimized for a specific exit temperature.

White et al. [49] found that, for a single charge operation, the temperature profile becomes progressively less steep as it moves through the reservoir and consequently the temperature difference between gas and solid (dashed lines) gradually decreases, thereby reducing the entropy generation rate. The sloping front constitutes a loss of stored available energy and prevents the reservoir from being fully charged without hot (or cold) gas first issuing from the exit, thereby incurring an exit loss.

Also the shape of the temperature profiles for cyclic operation (Figure 3.9b) depends on the length of the charge-discharge period relative to the time taken for an ideal (abrupt) thermal front to pass through the reservoir. Longer period cycles allow more energy to be stored but at the expense of steeper fronts and thus higher losses. It is worth pointing out that steady-state, periodic operation necessarily incurs an exit loss, as suggested by curve (iii) in Figure 3.9b, which shows the situation near the end of the charge phase and indicates the temperature at the exit of the reservoir beginning to rise. The exit loss reflects the need for heat to be rejected between successive cycles in order to counter the effects of irreversible heat transfer.

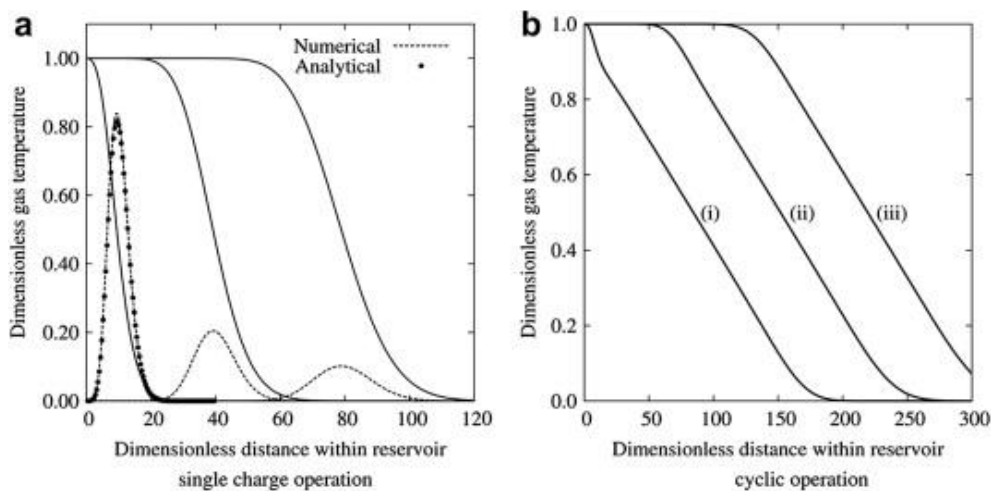


Figure 3.9: Reservoir temperature profiles for different modes of operation. See [22] for details.

A study by McTigue et al. [50] found that, to reach cyclic operation, a transient phase is passed through, during which it is established a balance between the entropy rejected at the exit of the store and the internal entropy generated by irreversibilities within the store. This balance leads to a trade-off between efficiency and energy density, where longer duration cycles store larger quantities of exergy at the expense of round-trip efficiency.

A numerical and theoretical analysis of thermal wave propagation in packed beds was performed by White et al. [51] and it showed that the temperature dependence of the solid specific heat capacity has a strong influence on the shape of temperature profiles, which is lower for cyclic operation than 'single charge', due to less abrupt thermal fronts. The main solution to mitigate the potentially large thermal losses was found to be avoiding the operation of the reservoirs in a mode that allows the shock-like features to form, so avoiding cold reservoirs from approaching a fully discharged state and hot reservoirs from becoming fully charged. The thermal front propagation in packed bed systems was found to lead also to unbalanced mass flow rates between the inflow and the outflow of packed beds. Their relation was investigated and validated experimentally by Wang et al. [45].

Depending on the operating conditions, stabilising the store exhaust temperature can be achieved by rejecting some heat from the fluid exiting the store to the environment or by adding some additional heat using an electric heater [38]. Although such control strategies can mitigate this problem, their use signifies that the packed-bed store is not utilised at its maximum potential and is thus required to be oversized, reducing the roundtrip efficiency.

In the work of White, McTigue and Markides [52] it was demonstrated that segmenting the thermal front into layers can significantly reduce the minimum loss that can be achieved. Segmented packed-bed storage has previously been proposed as a mean of retaining thermal stratification for solar applications. In the current context, is used to allow greater control of the thermal front and to divert the gas flow to pass only through active regions of the reservoir containing the thermal front, thereby reducing pressure losses. McTigue, Markides and White [50] explored the influence of the packed-bed store cycle duration on the roundtrip efficiency and stored exergy, concluding that, as already found by White [49], packed beds are more resilient to changes in available energy when the cycle duration is longer. Moreover, ending the charge/discharge cycles when a specific fluid exit temperature is reached can help to stabilise the performance. In a study by Albert et al. [33], elongating the tanks and increasing the segmentation temperature ratio was found to achieve a maximization of the duration of the high power region and decrease the size of the powerfront (sudden decrease of power) in CE device during discharge. The introduction of an additional latent storage allowed also the storage to completely discharge and a greater proportion of the stored energy to be returned as useful work. Therefore, this

solution was found to bring the LCOS below the value predicted for pumped hydro storage by Smallbone et al. [53].

Part-load operation of closed cycles can be achieved using ‘inventory control’ [36] where the volume of working fluid in the cycle is adjusted. The pressure on the low-pressure side is adjusted proportionally, so that the volumetric flow through the turbomachinery remains constant. The machines can then be operated over the same pressure ratio, and therefore maintain the same temperature ratio. Not only does this mean that energy can be stored and extracted at the design temperatures, but the efficiency of each machine remains close to its design efficiency. Inventory control requires a buffer vessel of working fluid. The volume of this vessel may be minimized by locating it where the working fluid density is highest. Zhao et al. [54] conducted an analysis of solid and liquid storage materials used in Brayton-cycle PTES systems, listing six different solid options and the main ones are reported in Table 3.4. These materials are in general abundant and cheap. Magnetite and hematite are convenient options as they can be used over a wide range of temperatures and their specific heat capacities experience relatively low variations with temperature.

Table 3.4: Main characteristics of sensible heat solid storage materials used in packed beds [54].

Storage material	Density $\rho$ [kg/m <sup>3</sup> ]	Specific heat capacity $c_p$ [J/(kg·K)]	Thermal conductivity $k$ [W/(m·K)]	Cost [\$/kg]
Magnetite (Fe <sub>3</sub> O <sub>4</sub> )	5081	851	4.91	0.5
Quartzite (SiO <sub>2</sub> )	2500	830	3.16	0.04
Alumina (Al <sub>2</sub> O <sub>3</sub> )	3990	1167	11.1	1.5
Titanium oxide (TiO <sub>2</sub> )	4230	692	8.40	1.7
Hematite (Fe <sub>2</sub> O <sub>3</sub> )	5240	628	12.6	0.5
Basalt	2640	1231	1.50	0.12

### 3.5.2. Liquid storage systems

Indirect liquid thermal storage tanks represent an alternative solution to packed-bed storage. The hot and cold storage require two separate tanks each and during charge the heat storage fluid is moved from one storage tank to another, being heated or cooled in the hot store and cold store respectively. Heat is transferred between the TES fluid and the working fluid via counter-current or co-current flow liquid-gas heat exchangers, as shown in Figure 3.10. In comparison to the packed-bed storage option, there are no thermal fronts, which means that the working fluid temperature at the inlet and outlet of the heat exchanger can be kept fixed. The liquid storage can be used at its full potential, so it can be fully charged and discharged. One of the main advantages is that, provided a suitable liquid, the liquid tanks do not have to be pressurised, allowing lower losses and costs, but working cycle can be pressurized to ten times the pressures of a packed bed, thus increasing the power density. The main disadvantage of this system however, is that the system requires four tanks in total and the equivalent volume of two tanks is always empty, so the energy density of this storage method can be lower than packed-bed systems.

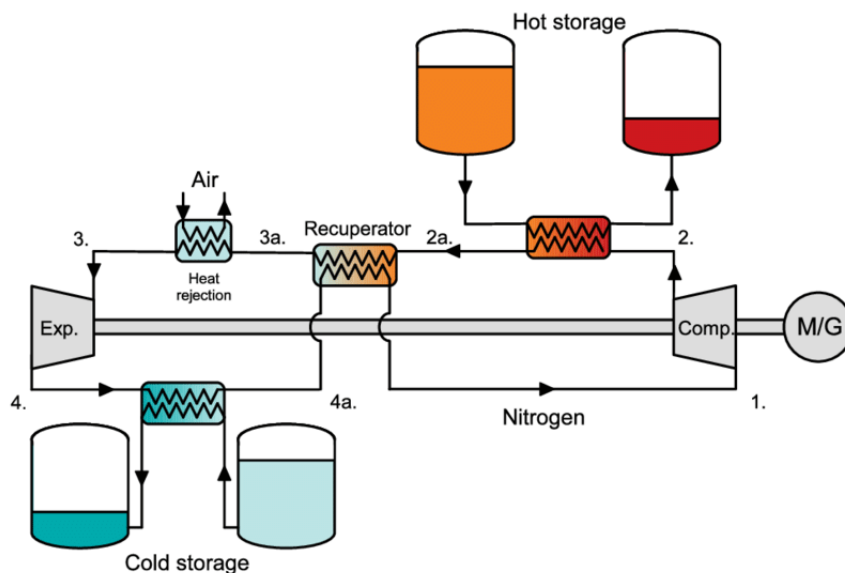


Figure 3.10: Layout of a liquid storage PTES system.

In comparison to solid materials, liquids are associated with smaller operating temperature ranges. For the hot liquid tanks, nitrate molten salts (Hitec, Hitec XL, solar salt, etc.) are often used, because they have desirable heat transfer characteristics and operating temperatures higher than 500 °C, being already used in concentrating solar

power plants. Temperature limits can be raised even higher to more than 700 °C, however this requires state-of-the art tank technology and high-performance steel.

At intermediate temperatures, synthetic fluids like Therminol 66, Therminol VP-1 or pressurised water are more suitable fluids. Furthermore, since most of the working temperature ranges of the above fluids overlap, different combinations of them are possible. For the cold tanks, organic liquids with working temperatures much lower than 0 °C can be deployed, for example butane, pentane, isopentane, propane and hexane. It is worth noting that most organic fluids are associated with additional drawbacks, like high global warming potential or flammability. Other options for cold storage are oxygen, nitrogen, ethanol, methanol or glycol water.

Since the temperature range of the two liquids is limited, a recuperator could be used. A regenerative heat transfer does not increase the roundtrip efficiency of the system, as mentioned by Laughlin[25], but recuperation has the benefit of reducing the pressure ratio, which not only reduces the number of compressor and turbine stages but also raises the coldest temperature of the cycle, thereby permitting a wider choice of cold storage fluids.

Many of the configurations proposed in literature used molten-salts for the liquid of the hot TES, with allowed temperature range of 290°C-565°C. For the cold TES Laughlin [25] used n-hexane, which is liquid at 1 bar from -95 to 77°C, while others, as Salomone-González et al. [39] used methanol, which at 1 bar is liquid from -98°C to 15 °C. In Table 3.5 are summarized the main characteristics of some of the most used liquid storage materials.

Table 3.5: Main characteristics of sensible heat liquid storage materials. The values of the thermophysical properties correspond to intermediate temperatures between  $T_{min}$  and  $T_{max}$  [54].

Storage material	$T_{min}$ [K]	$T_{max}$ [K]	Density $\rho$ , [kg/m <sup>3</sup> ]	Specific heat capacity $c_p$ , [J/(kg·K)]	Thermal conductivity $k$ , [W/(m·K)]	Cost [\$/kg]
HITEC	415	808	1637	1562	0.382	0.93
HITEC XL	403	823	1959	1432	0.519	1.43
Solar salt	533	873	1817	1517	0.525	0.5
Therminol 66	264	616	909	2072	0.109	1.0

Storage material	Tmin [K]	Tmax [K]	Density $\rho$ , [kg/m <sup>3</sup> ]	Specific heat capacity $c_p$ , [J/(kg·K)]	Thermal conductivity $k$ , [W/(m·K)]	Cost [\$/kg]
Therminol VP-1	285	673	909	2066	0.113	3.96
Rapeseed oil	280	523	843	2383	0.195	0.8
Pressurised water	273	486	896	4355	0.679	0.001
Butane (C <sub>4</sub> H <sub>10</sub> )	135	323	646	2139	0.136	1.0
Pentane (C <sub>5</sub> H <sub>12</sub> )	144	366	663	2141	0.129	1.0
Hexane (C <sub>6</sub> H <sub>14</sub> )	178	403	662	2240	0.123	1.0
Heptane (C <sub>7</sub> H <sub>16</sub> )	183	437	700	2292	0.119	1.0
Ethanol (C <sub>2</sub> H <sub>6</sub> O)	159	398	802	2292	0.168	1.0

McTigue et al. [46] proposed a techno-economic model of a recuperated PTES system with a two-tank liquid storage. The performance and cost of this system was shown to be strongly dependent on the heat exchanger design. A multi-objective optimization algorithm was used to evaluate the trade-off between LCOS and round-trip efficiency and to investigate the most suitable hot storage fluid. Results showed that the chloride salts configuration have lower values of LCOS and higher efficiencies than a system using nitrate molten salts. For example, the most cost-effective chloride salt system costs  $0,12 \pm 0,03$  \$/kWh<sub>e</sub> and has a round-trip efficiency of 60%, whereas the nitrate salt system achieves values of  $0,13 \pm 0,03$  \$/kWh<sub>e</sub> and 59%, respectively.

Some of the main storage configurations are reported in Table 3.6.

Table 3.6: Summary of different liquid TES configurations proposed in literature.

Authors	Hot store material	Cold store material	Number of tanks
Salomone-González et al. [39]	Molten salts	Methanol	2 HR, 2 CR
Zhao et al. [55]	High T (HT): solar salt Intermediate T (IT): Therminol 66	Butane	2 HR (HT and LT) 2 CR (HT and LT)
Gonzalez-Ayala et al. [56]	Molten salts	Anhydrous methanol	2 HR, 2 CR
McTigue et al. [46]	Nitrate molten salts	Methanol	2 HR, 2 CR
Yang et al. [47]	Nitrate molten salts	Methanol	2 HR, 2 CR
Chang et al. [57]	Molten salts	Refrigerant	2 HR, 2 CR

### 3.6. Compression and expansion machinery

For the compression and expansion of the working fluid during the charging and discharging processes of the Brayton-cycle PTES system, Saipem [28] and Malta Inc [31] used axial turbomachines, while Isentropic Ltd designed and patented reciprocating-piston devices [29]. The operation of turbomachines is based on the dynamic action of rotating blades, while positive-displacement (screw or reciprocating-piston) devices make fluids move by trapping a fixed amount of fluid and then forcing it into a discharge pipe. In practice, there are significant trade-offs between the two types of devices and the choice of the best type largely depends on the system application and size.

One of the main differences between positive-displacement and turbomachine devices is that the latter can only operate in one direction, which means that a turbomachinery-based PTES system based requires four machines, a pair of compressor and expander used during charging and a pair used during discharging.

Unlike turbomachines, positive-displacement devices are reversible by nature, for screw machines, or through adjusting valve timings, for reciprocating-piston devices. This means that a single device can be operated both as a compressor and an expander,



thus a PTES system using reversible compressors/expanders requires only two machines, one for the cold and one for the hot side. This is an intrinsic advantage of positive-displacement devices, as it means that system costs can be significantly reduced.

Positive-displacement devices can be associated with high pressure-ratio (>10) capabilities and robust part-load performance. Although not mature at such large scales, variable valve timing actuation technologies were shown to ensure an optimal operation of the reciprocating machines over a wide range of operating conditions, leading to high performance improvements in Brayton-cycle PTES systems (>35%) when compared to mechanically-actuated valve systems. In addition, the minimization of thermal and pressure losses often leads to piston designs with large bore-to-stroke length ratios [14]. Due to the above reasons, the use of positive-displacement machines in Brayton-cycle PTES systems requires, for the moment, the design of customised machines, which in the short-term means higher complexity and investment costs.

Moreover, they are likely to be more suitable for smaller power ratings (<5 MWe). However, a modular system could enable a device to achieve higher charging and discharging rates and, as these devices gain maturity, it is likely that the range of possible scales can be further extended. Isentropic Ltd began the construction of these machines, which was subsequently completed by Newcastle University, and the prototype devices reported achieved efficiencies in the range of 92%–94% [30].

Axial turbomachines instead are more cost-effective and efficient at larger power ratings (>50 MWe), therefore may be more suitable for high flow rates and larger-scale installations that are being developed in the near-term.

The efficiency of turbomachines peaks at a specific pressure and can be drastically affected by variations in part-load conditions. However, these devices involve less significant heat leakage losses and they are significantly more mature than positive-displacement machines. In fact, close-to-commercialised devices can be chosen, a solution which simplifies operation and maintenance issues, leading to reduced complexity in terms of design and installation, as well as leveraging decades-worth of cost and performance optimization.

Conventional turbomachines run in one direction, so they are either a compressor or an expander. While it may be theoretically possible to design a turbomachine that can run forwards (as a compressor) and backwards (and an expander), this will undoubtedly compromise the efficiency compared to two separate machines.

### 3.6.1. Reciprocating piston engine

A schematic diagram showing the working principle of a reciprocating compressor is represented in Figure 3.11. The compressor has a diameter  $d$  and a stroke length  $s = 2r_c$  (where  $r_c$  is the crank length), and rotates at an angular velocity  $\omega$ .

After compression, the valves, placed on the top of the piston, are opened and the flow is discharged until the piston reaches top dead centre (TDC). At this point the valves are closed and the piston reverses direction, thereby expanding the gas. The valves are then re-opened for the suction phase and closed again at bottom dead centre (BDC). In the absence of heat leakage and irreversibility the processes are isentropic.

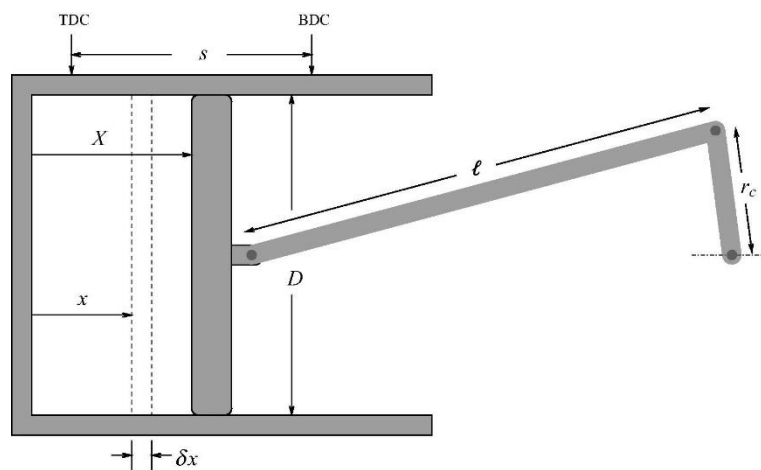


Figure 3.11: Scheme of a reciprocating device [58].

A new model for a reciprocating device was patented and developed by Howes and MacNaghten [29] for Isentropic Ltd.

The prototype, represented in Figure 3.12, was a piston, which comprised two faces, each with a dedicated piston ring working in a compression cylinder at the bottom and an expansion cylinder at the top. The faces were joined by a large number of vertical tie rods distributing the pressure loads across the piston faces and passing through a static heat exchanger. Passive reed valves were placed in the inlet face and lower (compression) piston face. Actively controlled reed valves were employed in the exhaust face and upper piston face for the expander. A new concept valve was developed and comprised a thin plate (typically less than 0.5 mm) perforated with a rectilinear array of small ports, which is depicted on the piston face in Figure 3.13.

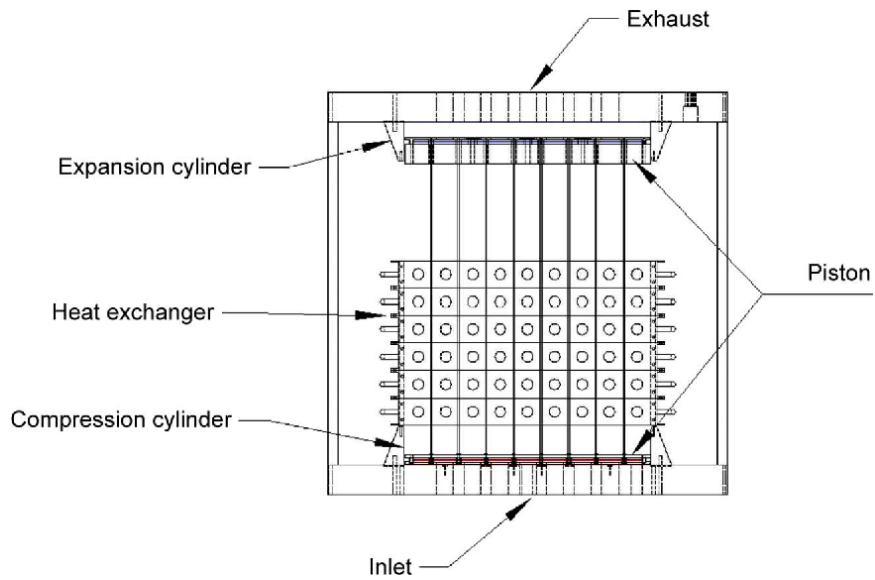
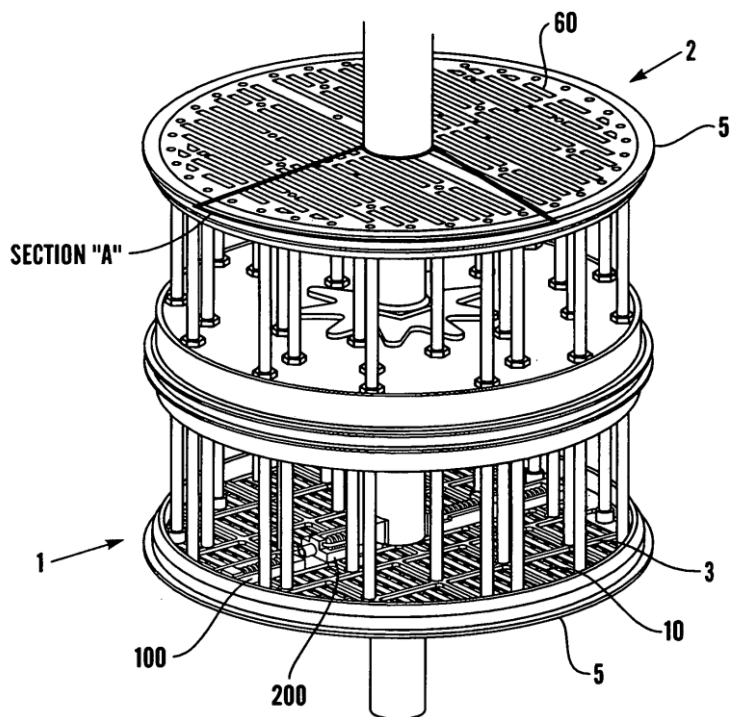


Figure 3.12: Section through working space of first prototype by MacNaghten and Howes [14].



**Fig. 1A**

Figure 3.13: Valve prototype by MacNaghten and Howes [30].

## 3.7. Other components

### 3.7.1. Heat exchangers

The heat exchangers present in a Brayton-cycle PTES system are auxiliary heat exchangers, gas heaters/coolers, evaporators/condensers and recuperators.

They are required for steady state cyclic operation to be achieved. They are typically placed at the outlet of the compression and expansion devices. These locations are closest to ambient temperature and are therefore the most efficient locations for heat rejection to occur.

Their design should consider a wide range of factors such as the required inlet and outlet temperatures of gas flow, the heat exchanger geometry (shell and tube, cross flow, multiple passes, fin shapes and sizes etc.), the gas or liquid and its mass flow rate, the desired performance and the economic cost of these design requirements. A simplified modelling considers two parameters: the effectiveness  $\epsilon$ , which governs the efficiency of the heat transfer processes, and a pressure loss factor  $f_p$ , which accounts for frictional pressure drops.

The most used are counter-current heat exchangers, with the commercialized ones achieving an effectiveness in the range of 92-97%.

### 3.7.2. Buffer vessel

A buffer tank is required by inventory control operation because the total mass of gas within the packed beds changes during charge, due to the variation of gas density at different temperatures. It gives some of the gas to the cycle or stores it to adjust proportionally the pressure on the low-pressure side, so that the volumetric flow through the turbomachinery remains constant.

The volume of this vessel may be minimized by locating it where the working fluid density is highest, so at the outlet of the hot store during charge may be the most suitable location as it is close to ambient temperature, which minimizes insulation requirements. However, pressure losses occur in the valves and pipes for both filling and emptying of the tanks.

### 3.8. Cost breakdown into components

The breakdown of costs of a Brayton-cycle PTES system into different components largely depends on the system design (cycle configuration, storage type, compression and expansion devices, etc.) and system size (rated discharge power and duration). Using the costing methodology from the work of Georgiou, Shah and Markides [59], the breakdown of costs of a system based on packed-bed thermal stores for four combinations of discharge power and duration is presented in Figure 3.14.

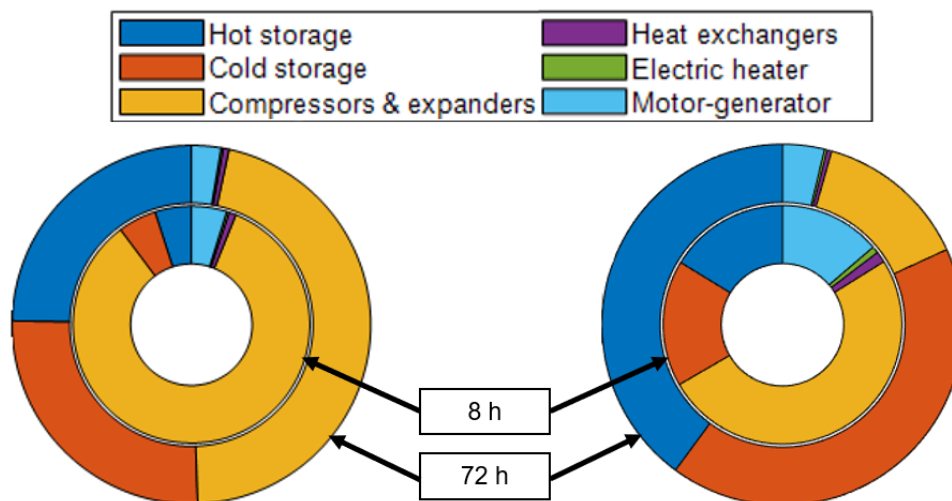


Figure 3.14: Breakdown of the investment cost of a Brayton-cycle PTES system based on packed-bed thermal stores into components for systems designed to provide a rated discharge power of: (a) 1 MW; and (b) 100 MW. Outer and inner rings represent costs for systems designed to have a discharge duration of 72 h and 8 h, respectively.

For systems with low discharge powers ( $< 1$  MW) the costs of compression and expansion devices dominate, while for systems with high discharge powers ( $> 100$  MW) the costs of hot and cold thermal stores are more significant. One of the reasons for this is that, although compression and expansion devices are expensive at small sizes, they experience significant economies of scale. For any rated discharge power, as the discharge duration increases from 8 to 72 h, the costs associated with the hot and cold thermal stores increase. The costs of thermal stores become higher than those associated with compression and expansion, especially for systems with high discharge power (100 MW) and high discharge durations (72 h).

### 3.9. Integration of PTES systems with other energy sources and sinks

An advantageous feature of PTES arises from its ability to manage different energy vectors (electricity, heat or cold energy).

Brayton-cycle PTES systems, as well as other storage systems based on thermo-mechanical concepts, can be associated with unique heat-electricity coupling features that distinguish them from other electricity storages. In fact, since electricity is stored in the form of pumped heat, additional waste-heat (from industrial processes) or renewable-heat sources can be integrated during charging, to reduce the amount of required electricity and improve the roundtrip efficiency. A solar-PTES hybrid system based on the integration of a concentrated solar power (CSP) plant and Brayton-cycle PTES system, represented in Figure 3.15 is proposed by Farres-Antunez, McTigue and White [60]. For instance, they suggested that a high-temperature heat pump using the Joule–Brayton cycle could be used to charge the molten-salt thermal stores at an existing CSP plant.

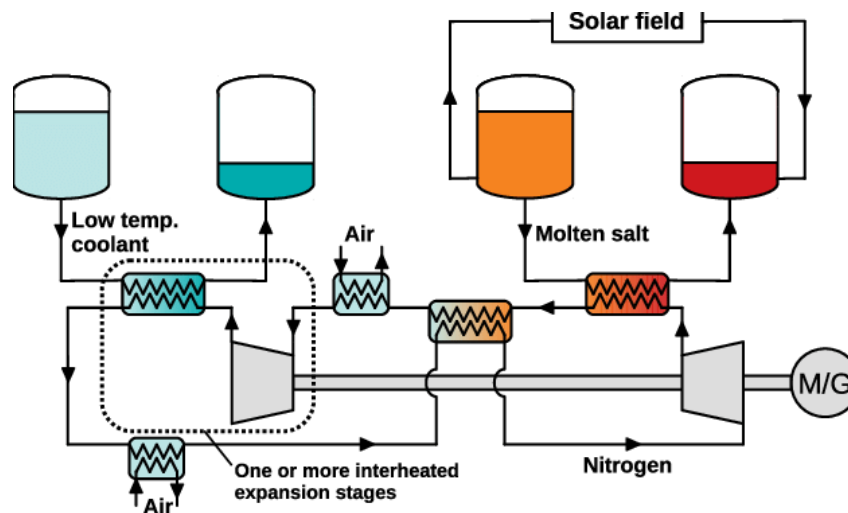


Figure 3.15: Layout of a new solar-PTES plant proposed by Farres-Antunez [60].

Charging might be not only needed to heat up the storage for later discharging, but might be also useful for cooling, for example in data centers or in manufacturing processes. If thermal energy at an elevated temperature from a waste-heat source is used to charge the storage system, the mechanical work needed in the charging process is reduced, thus improving the round-trip efficiency.

If the lowest temperature during discharging is sufficiently below the temperature of the waste-heat source used during charging, the electrical energy delivered during

discharging might even exceed the electrical energy used during charging. This is an interesting option for the utilization of low-temperature waste heat. During discharging, a PTES system might deliver both electrical energy and heat depending on the specific demand structure.

A novel combined cooling, heating, and power (CCHP) system based on Brayton-based PTES system was proposed by Zhang et al. [43]. Using an unsteady model established to simulate the system and explore its potential of energy storage and delivery, they found the system achieves a high COP, so it is very worthy of being practical applied.

Other projects have investigated how PTES may be integrated with a variety of thermal systems.

For example, a high temperature PTES (HT-PTES) based on an additional electric heater is proposed by Chen et al. [40] to enhance the energy storage capacity of PTES. Waste heat, which produced due to the irreversibility of heating, compression and expansion process of both PTES and HT-PTES, is recovered by the organic Rankine cycle (ORC) to generate power. Five types of PTES combined with ORC system namely, are investigated based on transient analysis method. The simulation results show that combined with ORC is an effective approach to improve the roundtrip efficiency (RTE) of both PTES and HT-PTES. In the five types of combined systems, the HT-PTES+parallel ORC is considered as a more promising large-scale energy storage technology, which main advantage is an acceptable RTE of 47.67%. Moreover, it shows appropriate operating pressures, which are 1.05 MPa for HT-PTES subsystem and 12.20 MPa for ORC subsystem, lower than the 31.2 MPa for ORC in the HT-PTES+ORC, and it presents a considerable energy storage density of 218.69 MJ/m<sup>3</sup>.

Brayton-cycle PTES system could also be potentially integrated with other TMES systems. In fact, Farres-Antunez et al. [26] proposed an advanced concept whereby a PTES topping cycle is integrated with a LAES bottoming cycle. By combining these cycles, the need for the cold liquid stores is removed, thereby reducing the required quantity of storage media and the cost per unit of energy capacity. Several configurations of the combined cycle were proposed, and they were found to have higher efficiencies and energy densities than either PTES or LAES. However, these advantages come with increased complexity and a higher cost per unit power, meaning that such combined cycles would be better suited to applications with medium/long charge/discharge duration times.

### 3.10. Optimization of system performances

The concepts developed by SAIPEM, Isentropic Ltd, and Malta Inc. provide an introduction to PTES systems based on Joule–Brayton cycles. Several other systems have been proposed in the literature, which propose either novel modifications or attempt to integrate PTES with other energy systems.

A first model of a Brayton cycle PTES, developed by Desrues et al. [23], was based on the Saipem scheme [28]. They proposed a PTES system with two tanks made of concrete bricks, in which the hot tank operates between a  $T_{\max} = 1012^{\circ}\text{C}$  (T2) and a  $T$  of  $25^{\circ}\text{C}$  (T3), while the cold tank works between  $500^{\circ}\text{C}$  (T1) and  $-70^{\circ}\text{C}$  (T4). The maximum pressure is 4,6 bar and the working fluid is argon.

A preliminary analysis presented by the authors tried to estimate the RTE for different maximum temperatures, introducing only turbomachinery irreversibilities, and as expected for a cycle with a low work ratio, they found the turbomachinery efficiency has a high influence on the RTE. They suggested that a RTE around 70 % could be obtained, with the lowest cost, by either employing a high maximum temperature and low turbomachinery efficiency or high turbomachinery efficiency and low maximum temperature. They developed a model for the packed bed, using a simplified geometry and considering only compression and expansion irreversibilities, with a polytropic efficiency of 0.9, and the irreversibilities due to the packed bed operation, like pressure drops and irreversibilities due to moving thermal front. They obtained a RTE of 66.7%, with a volumetric energy density of around  $28 \text{ kWh/m}^3$ , which is a value much higher than the energy density of pumped hydro energy storage. The heat exchangers have also another important function that is to keep the inlet temperature of turbomachinery constant during charge when the thermal front approaches the end of the vessel, that is also referred to as exit loss.

Moreover, since it is not convenient to cool a gas at high temperature, they proposed to change the discharge pressure ratio so that  $T1'$  is equal to  $T1'_{\text{nom}}$  and thus only to use one auxiliary heat exchanger, which works at quite lower temperature.

Ni and Caram [35] proposed a model with similar parameters to Desrues et al. [23], using exponential matrix solutions to investigate the cyclic steady state temperature distributions in the thermal reservoirs. They analyzed how dimensionless length and dimensionless charge period affect the roundtrip efficiency as well as the bed utilization ratio, which is the ratio of actual stored energy and the maximum amount of energy that can be stored in the PTES process. They found out that the RTE goes down if the tanks are used completely, for example if the hot tank is all brought to the maximum temperature. If only 50% of the packed bed is brought to the maximum temperature, with a  $\eta_{\text{pol}}=0.9$  they got a RTE of 72.2%. Moreover, they made an impact analysis of all losses on the RTE, including pressure and heat leakage losses (due to



non-ideal insulation of the reservoirs) and noticed that the optimal discharge pressure ratio is the one that allows an equal distribution of the exergy dissipated in the two auxiliary heat exchangers.

Howes [14] proposed a model based on the patent filed for Isentropic Ltd [29], using lower maximum temperatures of 500 °C and a pressure ratio of about 12 bar. A prototype of a piston-engine, with a new concept valve [30] [28], was used for this 2 MW configuration and, considering several losses, a roundtrip efficiency of 72% was achieved for a full charge-discharge cycle.

The first demonstration of PTES facility was built by the company known as Isentropic Ltd, based on the patent of MacNaghten and Howes [29], and it was then handed over to the Sir Joseph Swan center at Newcastle University to commission and test the facility. The system has a storage capacity of 600 kWh and a rated output power of 150 kW and proprietary reversible compression and expansion equipment with a pressure ratio of 12. The working fluid passes directly through the thermal stores and the hot thermal store is a pressure vessel capable of withstanding 12 bar and a temperature of 773 K. In 2019 successful demonstration of a turn-round efficiency of 65% was reported in this first of a kind system.

Smallbone et al. [53] presented an economic analysis of a PTES system using data obtained during the development of the grid-scale demonstrator project by Newcastle University. The LCOS for the PTES system with a demonstrator size of 2 MW power and a capacity of 16 MWh ranged between 0.07 and 0.11 €/kWh.

Isentropic Ltd configuration was taken as reference by many works, for example White [49], who analyzed thermodynamic losses in thermal reservoirs due to irreversible heat transfer and frictional effects, and White et al. [22], who presented a sensitivity of roundtrip efficiency to various loss parameters, indicating particular susceptibility to compression and expansion irreversibility.

McTigue et al. [21] used similar parameters and plant size as Howes [14] to develop a steady flow analysis of the compression and expansion devices coupled with a Schumann-style model of the hot and cold thermal stores. Parametric studies revealed that there are optimum values for some design variables, while others lead to a trade-off between efficiency and energy density. Multi-objective optimisation has been applied to generate trade-off surfaces, known as Pareto fronts, and these show that curves of roundtrip efficiency versus energy density are relatively flat over a considerable range, so that high energy density can be attained with only a modest efficiency penalty.

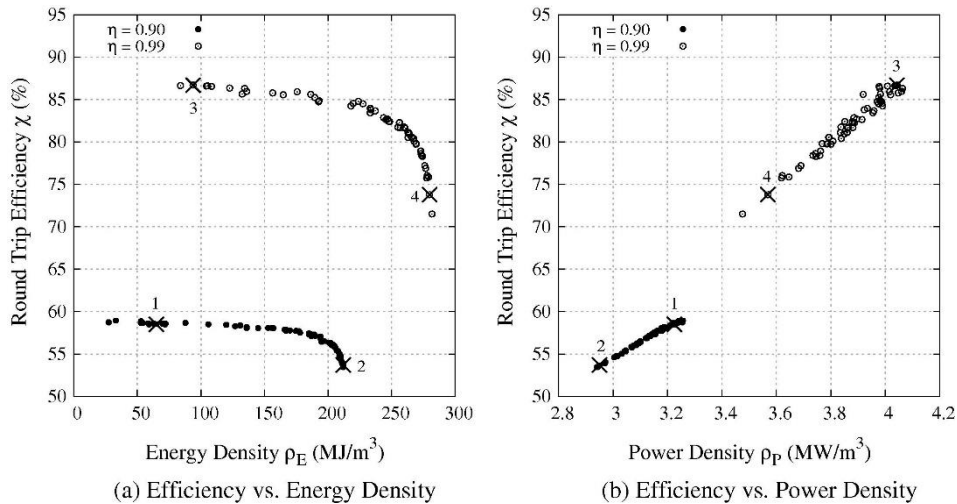


Figure 3.16: Pareto fronts (trade-off surfaces) from the optimisation by McTigue et al. [21].

It was found that, with reasonable estimates for mechanical and electrical losses, this would give an overall roundtrip efficiency of just under 70%, with the use of high-efficiency reciprocating devices. On the other hand, if the compressors and expanders could achieve efficiencies typical of turbomachinery, then the overall roundtrip efficiency is unlikely to exceed 50%.

The results of another study by McTigue et al. [50] on the performance response of packed bed to cycle duration perturbations also demonstrated that the cycle performance for specific compression and expansion efficiencies was controlled chiefly by the ratio between the highest and lowest temperatures in each reservoir rather than by the cycle pressure ratio.

The cyclic transient behavior of a 10 MW/4 h PTES was investigated by Wang et al. [36], and showed that the delivery power declines during the discharging process, mainly due to the thermal energy reduction from the packed bed TES reservoirs. The analysis also found that for TES reservoirs exist optimal selections of particle sizes, ratios of length-to-diameter and discharging durations corresponding to the maximum round-trip efficiency and preferable discharging power stability. This is mainly owing to the joint effects of the pressure loss, heat transfer and thermodynamics.

A similar configuration, but with a discharge duration of 8 h, was investigated by Wang et al. [44] to numerically simulate the cyclic steady-state transient behavior under four operation modes, which are series, parallel, in-sequence, and the innovative “temperature complementation”, as well as reservoir numbers of three, five, and seven. The PTES with series-connected reservoirs arrays has a round-trip efficiency of 64.9% and a delivery variation of 43.1%; these results are better than those obtained under the parallel and in-sequence operating modes of the singular reservoir. Under the innovative “temperature complementation” operation mode, the delivery

stability improves further with a variation of 13.2%. The TES reservoirs could be reduced to 1.8 times the minimum volume with a round-trip efficiency of 63%–65%.

The problem of unbalanced mass flow rates between the inflow and the outflow in packed beds was investigated by Wang et al. [45]. They discussed the sensitivities of factors such as pressure ratio, heat capacity of TES material and porosity on the unbalanced mass flow rate and the round-trip efficiency of the system, considering mass flow rate. Results showed that a self-balancing PTES system, without buffer vessel, has a round-trip efficiency 0.12% higher than the buffer vessel balancing one, avoiding also the buffer tank costs.

The relevant influencing factors, such as the pressure ratio, polytropic efficiency, particle diameters and structures of thermal energy storage reservoirs, were also analysed. The results indicated that helium (He) with a roundtrip efficiency of 57% presented an advantage over argon (Ar) with an efficiency of 39%.

Benato [38] added an electric heater to the charging phase of a PTES system with the aim of maintaining the plant maximum temperature at constant value, so that this parameter is not affected by the compressor pressure ratio as in previous configurations. The discharging cycle is the same as a conventional PTES cycle. This system achieved a round-trip efficiency of 9.5% at maximum storage temperatures of 1050 °C. This low value is partly due to the heater reducing the heat pump coefficient of performance, and partly because the thermal stores are 'unbalanced'; the heater increases the energy stored in the hot store without any increase in the energy stored in the cold store. As a result, the cold store discharges more quickly than the hot store, and not all of the hot energy can be extracted from the cycle. The proper storage material and its shape are also important parameters. The higher the cycle maximum temperature, the higher the stocked energy and the lower the specific costs.

The results revealed that the roundtrip efficiency peaked (27%) at a temperature of 950 °C with air as the working fluid. If the grid required high power for a short period of time (lower than 3 h), storages made of concrete spheres could be adopted; if the requirement was high power for a long period of time (4-5 h), hematite (Fe<sub>2</sub>O<sub>3</sub>) or magnetite (Fe<sub>3</sub>O<sub>4</sub>) could be used.

A similar system was proposed by Chen et al. [40], who aimed to extract this excess heat using an additional engine during discharge. Incorporating an ORC system was found to improve the round-trip efficiency to 47.7%, which is similar (although slightly lower) than a PTES system operating at lower temperatures without the electric heater (47.9%).

A comparison between a coupled and a decoupled packed bed PTES system was made by Davenne et al. [34]. The outline system was designed to be capable of delivering 1 GWh of stored electric energy with a predicted achievable roundtrip efficiency of 59.5%. A performance and simple cost comparison showed that decoupling the thermal stores avoids the complexity and significant cost of pressure vessels, thus

rendering the decoupled concept highly scalable. However, losses associated with the thermal stores are found to be of the order of 2% in the coupled case, while in the decoupling case are of the order of 10%.

The thermodynamic feasibility of a packed bed system using latent heat/cold stores was explored by Ge et al. [37] to replace the sensible one. A numerical model of a 10.5 MW/5 h storage system was established, carrying out the energy and exergy analysis of components and investigating optimal conditions. It is concluded that the energy storage density of the system increases from 232.5 kWh/m<sup>3</sup> to 245.4 kWh/m<sup>3</sup>, when packed bed sensible stores are replaced by latent ones. Furthermore, the power density of the system is 216.5 kW/m<sup>3</sup> and the round-trip efficiency reaches 84.7%.

The integration of additional latent storage into a packed bed PTES cycle was also investigated by Albert et al. [33] and was found that it could improve system roundtrip efficiency up to 80%, using isentropic reciprocating compressors and expanders. The objective was to maximise the duration of the high power region and decrease the width of the power front. Moreover, the addition of latent storage could bring the LCOS of the system below the value predicted for pumped hydro storage.

PTES off-design and part-load performances are estimated in a study by Frate et al. [61], which investigated the impact of packed-bed behavior on turbomachines operating conditions. A control strategy especially suited for closed Brayton cycles, known as the inventory control (IC), is used, resulting in good part-load performance, which might be a significant advantage over the competing technologies. However, the off-design condition induced by the packed bed thermal behavior might significantly reduce the system performance and, in particular, that of the discharge phase. Therefore, it was found that the use of reduced discharging phase durations or oversized packed beds could help avoiding the efficiency reduction.

The first liquid storage configuration, proposed by Laughlin for Malta Inc [25], analyzed the performances of a system using solar salt and hydrocarbons, like methanol, for hot and cold storages, respectively. The author highlighted that, due to practical material limitations, heat transfers on the high-pressure and low-pressure sides of the circuit may overlap, thus eliminating the need to actually transfer heat to or from the storage fluids over this temperature range. In this case a gas-gas heat exchanger called regenerator or recuperator can be used. In the limit that the entropy generation by the heat exchangers is zero, regeneration has no effect at all on the round-trip efficiency but simply reduces the amount of heat exchanger steel required. It also reduces the temperature ranges over which the storage fluids are required to be liquid.

A thermodynamic model for a steady state pumped heat energy storage in liquid media is presented by Salomone-González et al. [39]. The model considers non-isothermal heat transfers between the working fluid and the liquid media and includes

a set of parameters accounting for the main internal and external losses, heat leak, and pinch point effects for both the heat pump and heat engine modes. Round trip efficiencies around of 35-40% have been obtained, internal losses being those with main negative influence on the calculated values.

The same authors presented a multi-objective and multi-parametric optimization of a PTES system by the calculation of different Pareto fronts. Round-trip efficiencies in the so-called optimum scale/mass-flow-ratio design point exhibit larger values compared to previously reported results including the so-called endoreversible limit, where no internal irreversibilities are considered and where the improvement can achieve 49% over the endoreversible case in the most ideal scenario.

An advanced exergy analysis of a recuperated liquid thermal stores system was performed by Zhao et al. [55]. Results of the recuperated system indicate that the expander during discharge is associated with the maximum exergy destruction rate (13%). The advanced exergy analysis further reveals that the cold heat exchanger during discharge is associated with the highest share (95%) of the avoidable exergy destruction rate, while during charge the same component is associated with the highest share (64%) of the endogenous exergy destruction rate. Thus, the cold heat exchanger offers the largest potential for improvement in the overall system exergetic efficiency.

A techno-economic model of a two-tank liquid storage system based on a recuperated cycle was proposed by McTigue et al. [46]. Models have been developed for each component, with particular emphasis on the heat exchangers.

It is found that the use of heat exchangers with effectiveness up to 0.95 is economically worthwhile, but higher values lead to rapidly escalating component size and system cost. Several hot storage fluids are considered. Those operating at the highest temperatures (chloride salts) improve the round-trip efficiency, but the benefit is marginal and may not warrant the additional material costs and risk when compared to lower-temperature nitrate salts. Cost-efficiency trade-offs are explored using a multi-objective optimization algorithm, yielding optimal designs with round-trip efficiencies in the range 59-72% and corresponding levelized storage costs of  $0.12 \pm 0.03$  and  $0.38 \pm 0.10$  \$/kWh<sub>e</sub>.

Farres-Antunez et al. [26] proposed a combined system in which PTES operates as a topping cycle and LAES as a bottoming cycle. The fundamental advantage is that the cold thermal reservoirs, which would be required by the two separate cycles, are replaced by a single heat exchanger between them, saving significant amounts of storage media per unit of energy stored.

A thermodynamic study of a baseline configuration of the combined cycle is presented and results indicate that the new cycle has a similar round-trip efficiency to that of the separate systems, while providing a significantly larger energy density. Furthermore, three adaptations of the base-case combined cycle are proposed and optimised. The

best of these adaptations achieves an increase in thermodynamic efficiency of about 10 percent points (from 60% to 70%), therefore significantly exceeding the individual cycles in both energy density and efficiency.

A solar-PTES concept, presented by Farres-Antunez et al. [60], analyzed the layout and numerical models of two different solar-PTES schemes, one in which a conventional CSP plant (based on the steam cycle) is retrofitted with a Brayton heat pump, and another one in which the Brayton cycle is used both during charge and discharge.

The results from the numerical model indicate that, in the two schemes, heat-to-work efficiencies of around 40% (in CSP operation) and round-trip efficiencies of around 55-60% (in PTES operation) can be achieved with state-of-the-art components.

Another PTES system thermally integrated with a Concentrating Solar Power (CSP) plant is proposed by Petrollese et al. [62]. A Thermal Energy Storage (TES) system composed of three thermocline packed-bed tanks is included. As a case study, an integrated PTES-CSP system characterized by a nominal power of 5 MW with a nominal storage capacity of 4 equivalent hours was considered.

The results demonstrated that the exergetic roundtrip efficiency of the integrated plant reaches a maximum for a pressure ratio of about 5.2. Finally, a feasible design for the PTES-CSP system characterized by an exergetic roundtrip efficiency of about 60% was proposed.

Table 3.7: Summary of Brayton-cycle PTES models proposed in the literature with key parameters.

Authors	Max/min T [°C]	$\beta_c - \beta_D$ ( $P_2/P_1$ ) [-]	$\tau =$ $T_2/T_1$ [K/K]	$\theta =$ $T_3/T_1$ [K/K]	Plant size MW/MWh	RTE [%]	Energy density [kWh/m <sup>3</sup> ]	Additional data]
Desrués et al. [23]	1000/-70	4,6	1268 / 773 = 1,64	298 / 573 = 0,52	100 / 602,6	66,7 (theo.)	27,86	TES: concrete bricks
Howes [14]	500/-166	12	-/-	~1	2 / 16	72	44,8	Rec engine prototype
McTigue et al. [21]	505/-150	10 (10,5 / 1,05)	778 / 310 = 2,5	310 / 310 = 1	2 / 16	~70	~50	Model opt. trade-off
Ni and Caram [35]	1000/-70	3-3,88	~1,6	298 / 773 = 0,386	-	64 (Ar)	-	Losses of thermal front

Benato [38]	550/-70	6	823 / 298 = 2,76	1	1,7 / 2,72 (1,6 h dis.)	6,34	70 - 430	5 storage materials
Davenne et al. [34]	727/-173	20	1000 / 300 =	300 / 300 = 1	100 / 1000	59,5 (63,4 dir.)	-	Indirect / direct storage
Zhao et al. [55]	505/-150	~10	-	-	10 / 60	57 (1) 54 (2)	-	1: $\eta_{is}=0,95$ 2: $\epsilon_{HX}=0,98$
Wang et al. [44]	505/-150	10 (1,05 / 0,105)	778 / 310 = 2,5	310 / 310 = 1	10 / 80	64,9	-	TES array of 3, 5 and 7 tanks
Ge et al. [37]	501/-145	10	-	298 / 298 = 1	10,5 / 52,5	84,7	245,4	Exergy analysis
Zhang et al. [41]	515/-145	10 (1,05 / 0,105)	-	298 / 298 = 1	10 / 40	65	26	Ind./dir. system compar.
Albert et al. [33]	450/-159	10	717 / 281 = 2,55	298 / 298 = 1	1 / 4	~80	-	Additional latent storage
McTigue et al. [46]	565/	10 (25 / 2,5)	838 / 573 = 1,46	298 / 573 = 0,52	100 / 1000	53	15	Recup. cycle
Petrollese et al. [62]	727/-100	5,2 (5,2 / 1)	-	-	5 / 20	60,4 (exer.)	-	Integrated PTES-CSP plant

### 3.11. Thermo-economic analysis

Brayton-cycle PTES systems are still at the development stage and several components are not commercially available.

Analysing their financial feasibility and competitiveness requires an estimate of the costs based on existing component cost surveys and literature data. Georgiou, Shah and Markides [59] conducted a techno-economic comparison of Brayton-cycle PTES and LAES, however they noted that it is not known which costing method in the

literature is the most accurate and different costing techniques lead to remarkably different estimates. To reduce these uncertainties, the authors used mean cost estimates for all components from multiple costing approaches based on the module costing technique by Turton et al. [63].

Following a similar approach, Olympios et al. [13] conducted a comprehensive review of promising thermo-mechanical energy storage technologies, estimating and comparing the component and system costs of the main TMES options for a large range of possible discharge power ratings and discharge durations.

They highlighted that, for all technologies, as the rated discharge power rating increases, the power and energy capital costs reduce significantly. On the other hand, as the discharge duration increases, the power capital cost increases, since the same power is provided using a larger store; and the energy capital cost reduces, as any costs associated with power-related technologies (compressors and expanders) remain constant.

Figure 3.17 can be used as a benchmark for estimating the power capital cost (total system cost over rated discharge power) and energy capital cost (total system cost over rated discharge energy capacity) of packed-bed and liquid storage Brayton-cycle PTES systems, respectively. The maps proposed are based on a specific set of design assumptions, which are: for all considered sizes, the compression and expansion polytropic efficiencies have been assumed to be equal to 90%, the heat exchanger effectiveness equal to 95%; and for large components, multiple units are assumed to be installed in parallel. Figure 3.17c,d correspond to the concept proposed by McTigue et al. [21], while Figure 3.17a,b correspond to the concept of Malta Inc [25].

Systems based on packed-bed thermal stores have higher power and energy densities, so they show slightly lower power and energy capital costs than systems based on liquid-tank thermal stores. This is mainly because liquid-tank systems require four separate tanks, two on each side. This means that the equivalent volume of two tanks is always empty when fluid is moved from one tank to another, so the energy and power densities and thus the energy and power capital costs are lower than packed-bed systems. However, the design of a large-scale system based on liquid tanks is significantly less complex than one based on pressurized packed-bed stores, so that means that the former is more likely to appear in slow discharge PTES designs.



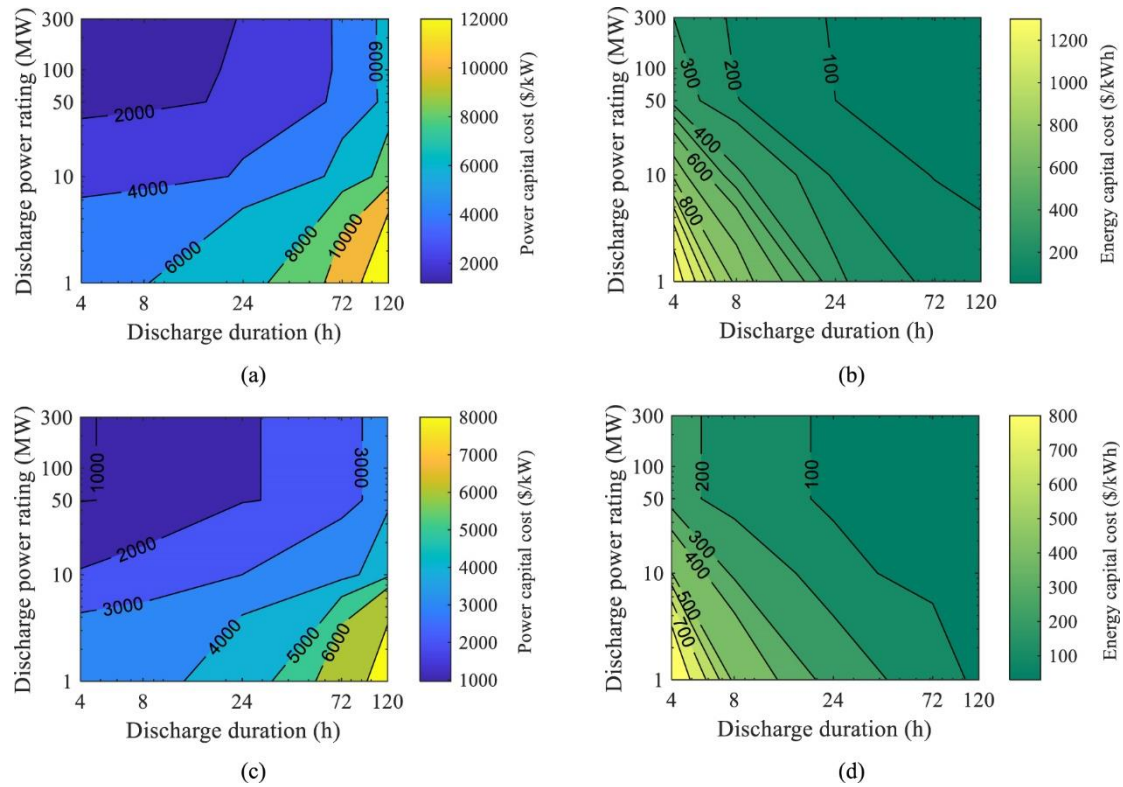


Figure 3.17: Thermo-economic analysis of two PTES systems based on Joule–Brayton cycle for varying discharge power rating and discharge duration: (a) power capital cost for a system with liquid-tank TES; (b) energy capital cost for a system with liquid-tank TES; (c) power capital cost for a system with packed-bed TES; and (d) energy capital cost for a system with packed-bed TES. The plots are logarithmic on both axes [13].

## 4 Comparisons and final considerations

Many authors developed different expressions, based on the chosen modelling approach, to estimate the roundtrip efficiency and analyzed other metrics that can be used to assess the system performance, as well as their relationships with roundtrip efficiency. The different assumptions proposed led to different results in the performance optimization.

The thermodynamic model proposed by Desrues et al. [23] first showed, through sensitivity analyses, the importance of efficiencies of compressors and expanders for high RTE and described the influence of loss parameters, which depend on detailed design, on system performances. Although the models were not very accurate, due to ideal heat transfer and no heat leakage assumptions, the results showed the feasibility of the process, even with sub-optimal parameters.

An area in particular need of further investigation is the development of higher efficiencies reciprocating devices, as the one presented by Howes [14], minimising heat-transfer losses, mass leakage and pressure losses through the valves, which in the short-term mean higher complexity and investment costs.

Parametric studies conducted by White et al. [21] revealed that there are optimum values for some design variables for PTES, while others lead to a trade-off between efficiency and energy density. Multi-objective optimisation has been applied to generate trade-off surfaces known as Pareto fronts. In the optimised designs, losses associated with pressure drop and irreversible heat transfer in the stores are only a few percent, so the success of PTES is likely to hinge upon compressor and expander performance. Further parametric studies by Salomone-González et al. [39] showed that it is not possible to simultaneously optimize power output and round-trip efficiency.

Ni and Caram [35] used a simplified discretized heat transfer model to simulate a PTES configuration similar to the one by Desrues [23]. The exponential matrix solution was used for a first principle analysis, showing the effects of heat transfer resistance and turbomachinery efficiency on the process performance. However, this approach isn't available when considering the dynamic process of the system pressure change and dependence of heat capacity and heat transfer coefficient on temperature, pressure and Reynolds number.

Some studies proposed also the use of an electric heater [38] to maintain the maximum temperature at a constant value, but this resulted in a poor RTE due to high energy losses, as confirmed by other works. However, the author investigated five types of storage material and two storage material shapes, showing the impact on improving energy density and reducing specific costs.

Another important issue to be tackled is the unbalanced mass flow rate between the inflow and the outflow of packed beds. The analysis performed by Wang et al. [45] however, indicates that the self-balancing PTES system will not only improve the 0.12% of round-trip efficiency but also save the initial cost by voiding the components including the BV, pressure pipelines, valves and their controllers.

Studies on the cyclic transient behavior, like the one by Wang et al. [36], highlighted that for TES reservoirs exist optimal selections of particle sizes, ratios of length-to-diameter, and discharging durations, corresponding to the maximum round-trip efficiency and preferable discharging power stability. This is mainly owing to the joint effects of the pressure loss, heat transfer and thermodynamics.

Many authors underlined the need to further investigate the optimization of heat exchange in the thermal stores through numerical models.

A large size decoupled system proposed by Davenne et al. [34], developing a multi-dimensional numerical study of the thermal stores, is advised to check that the 1D method and assumptions used are reasonable for very large, low aspect ratio thermal stores. Future work should include a design study of adiabatic turbomachinery.

Arrayed multimodular packed bed TES reservoirs may be a more promising TES option than singular large reservoirs, as underlined by Wang et al. [44].

The segmentation of packed beds was found to improve the efficiency and the integration of an additional latent storage was proposed by Albert et al. [33], but lack of data surrounding the transient properties of the PCMs is suggested to be a limitation of this study.

Many studies on liquid storage configurations [39], [56] considered the use of a regenerator in order to improve the efficiency, but their coupling with the heat exchangers have to be confronted with a detailed techno-economic analysis. An exergy analysis of a liquid storage recuperated system by Zhao et al. [55] showed the importance of heat exchangers efficiency.

It was found that thermal energy storage in the form of packed beds of solids is associated with higher energy density than liquid tank storage. However the heat transfer process in the former entails many constructive complexities, such as the need to pressurize the tanks, which brings high cost materials. Also round-trip efficiencies seem to be slightly higher in the former case, which is mainly due to the direct contact heat exchange, while in the latter case is reduced by the heat transfer in the de-coupling heat exchangers [41].

A promising solar-PTES is presented by Farres-Antunez [60] as a new concept of a hybrid system that combines concentrated solar power (CSP) and PTES. The results from the numerical model indicate that, in the two schemes, heat-to-work efficiencies of around 40% (in CSP operation) and round-trip efficiencies of around 55–60% (in PTES operation) can be achieved with state-of-the-art components. Future work will investigate the effect of incorporating cold storage tanks to boost the efficiency of the steam plant within the CSP-retrofit scheme.

The advanced concept proposed by Farres-Antunez et al. [26], where a PTES topping cycle is integrated with a LAES bottoming cycle, showed a reduced quantity of storage media required and a reduced cost per unit of energy capacity. Several configurations of the combined cycle were proposed, and they were found to have higher efficiencies and energy densities than either PTES or LAES. However, these advantages come with increased complexity and a higher cost per unit power, meaning that such combined cycles would be better suited to applications with medium/long charge/discharge duration times.

## Bibliography

- [1] “IPCC – Intergovernmental Panel on Climate Change.” <https://www.ipcc.ch/> (accessed Jun. 28, 2023).
- [2] “A European Green Deal.” [https://commission.europa.eu/strategy-and-policy/priorities-2019-2024/european-green-deal\\_en](https://commission.europa.eu/strategy-and-policy/priorities-2019-2024/european-green-deal_en) (accessed Jun. 27, 2023).
- [3] “Renewable electricity growth is accelerating faster than ever worldwide, supporting the emergence of the new global energy economy - News - IEA.” <https://www.iea.org/news/renewable-electricity-growth-is-accelerating-faster-than-ever-worldwide-supporting-the-emergence-of-the-new-global-energy-economy> (accessed Jun. 27, 2023).
- [4] “Renewable Energy Market Update - May 2022 – Analysis - IEA.” <https://www.iea.org/reports/renewable-energy-market-update-may-2022> (accessed Jun. 27, 2023).
- [5] IRENA, “Innovation Outlook: Thermal Energy Storage,” *International Renewable Energy Agency, Abu Dhabi*, p. 144, 2020, Accessed: Jun. 27, 2023. [Online]. Available: <https://www.irena.org/publications/2020/Nov/Innovation-outlook-Thermal-energy-storage>
- [6] A. Benato and A. Stoppato, “Pumped Thermal Electricity Storage: A technology overview,” *Thermal Science and Engineering Progress*, vol. 6, pp. 301–315, Jun. 2018, doi: 10.1016/J.TSEP.2018.01.017.
- [7] M. Aneke and M. Wang, “Energy storage technologies and real life applications – A state of the art review,” *Appl Energy*, vol. 179, pp. 350–377, Oct. 2016, doi: 10.1016/J.APENERGY.2016.06.097.
- [8] A. Gil *et al.*, “State of the art on high temperature thermal energy storage for power generation. Part 1 – Concepts, materials and modellization,” *Renewable and Sustainable Energy Reviews*, vol. 14, no. 1, pp. 31–55, Jan. 2010, doi: 10.1016/J.RSER.2009.07.035.
- [9] “World Energy Council | World Energy Council.” <https://www.worldenergy.org/> (accessed Jun. 27, 2023).
- [10] M. Budt, D. Wolf, R. Span, and J. Yan, “A review on compressed air energy storage: Basic principles, past milestones and recent developments,” *Applied Energy*, vol. 170. Elsevier Ltd, pp. 250–268, May 15, 2016. doi: 10.1016/j.apenergy.2016.02.108.

- [11] "Home | Highview Power." <https://highviewpower.com/> (accessed Jun. 27, 2023).
- [12] X. Luo, J. Wang, M. Dooner, and J. Clarke, "Overview of current development in electrical energy storage technologies and the application potential in power system operation," *Appl Energy*, vol. 137, pp. 511–536, Jan. 2015, doi: 10.1016/J.APENERGY.2014.09.081.
- [13] A. V. Olympios *et al.*, "Progress and prospects of thermo-mechanical energy storage-a critical review," *Progress in Energy*, vol. 3, no. 2. Institute of Physics, Mar. 12, 2020. doi: 10.1088/2516-1083/abdbba.
- [14] J. Howes, "Concept and development of a pumped heat electricity storage device," in *Proceedings of the IEEE*, Institute of Electrical and Electronics Engineers Inc., 2012, pp. 493–503. doi: 10.1109/JPROC.2011.2174529.
- [15] A. Thess, "Thermodynamic efficiency of pumped heat electricity storage," *Phys Rev Lett*, vol. 111, no. 11, Sep. 2013, doi: 10.1103/PhysRevLett.111.110602.
- [16] M. Mercangöz, J. Hemrle, L. Kaufmann, A. Z'Graggen, and C. Ohler, "Electrothermal energy storage with transcritical CO<sub>2</sub> cycles," *Energy*, vol. 45, no. 1, pp. 407–415, Sep. 2012, doi: 10.1016/J.ENERGY.2012.03.013.
- [17] A. Vecchi *et al.*, "Carnot Battery development: A review on system performance, applications and commercial state-of-the-art," *J Energy Storage*, vol. 55, p. 105782, Nov. 2022, doi: 10.1016/J.EST.2022.105782.
- [18] P. Farrés Antúnez, "Modelling and development of thermo-mechanical energy storage," 2018.
- [19] M. Abarr, B. Geels, J. Hertzberg, and L. D. Montoya, "Pumped thermal energy storage and bottoming system part A: Concept and model," *Energy*, vol. 120, pp. 320–331, Feb. 2017, doi: 10.1016/J.ENERGY.2016.11.089.
- [20] J. Mctigue, "ANALYSIS AND OPTIMISATION OF THERMAL ENERGY STORAGE," 2016.
- [21] J. D. McTigue, A. J. White, and C. N. Markides, "Parametric studies and optimisation of pumped thermal electricity storage," *Appl Energy*, vol. 137, pp. 800–811, Jan. 2015, doi: 10.1016/J.APENERGY.2014.08.039.
- [22] A. White, G. Parks, and C. N. Markides, "Thermodynamic analysis of pumped thermal electricity storage," *Appl Therm Eng*, vol. 53, no. 2, pp. 291–298, May 2013, doi: 10.1016/J.APPLTHERMALENG.2012.03.030.
- [23] T. Desrues, J. Ruer, P. Marty, and J. F. Fourmigué, "A thermal energy storage process for large scale electric applications," *Appl Therm Eng*, vol. 30, no. 5, pp. 425–432, Apr. 2010, doi: 10.1016/J.APPLTHERMALENG.2009.10.002.

- [24] J. Guo, L. Cai, J. Chen, and Y. Zhou, "Performance optimization and comparison of pumped thermal and pumped cryogenic electricity storage systems," *Energy*, vol. 106, pp. 260–269, Jul. 2016, doi: 10.1016/J.ENERGY.2016.03.053.
- [25] R. B. Laughlin, "Pumped thermal grid storage with heat exchange," *Journal of Renewable and Sustainable Energy*, vol. 9, no. 4, Jul. 2017, doi: 10.1063/1.4994054.
- [26] P. Farres-Antunez, H. Xue, and A. J. White, "Thermodynamic analysis and optimisation of a combined liquid air and pumped thermal energy storage cycle," *J Energy Storage*, vol. 18, pp. 90–102, Aug. 2018, doi: 10.1016/J.EST.2018.04.016.
- [27] B. Weissenbach, "Thermal energy storage device," EP0003980A1, 1979
- [28] J. Ruer, "Installation and methods for storing and recovering electric energy," WO2008148962A2, 2008
- [29] J. MacNaghten and J. S. Howes, "Energy storage," WO2009044139A2, 2009
- [30] J. MacNaghten and J. S. Howes, "Valve," EP2220410B1, 2010
- [31] R. B. Laughlin, "Systems and methods for energy storage and retrieval," US20150260463A1, 2015
- [32] R. B. Laughlin, "Adiabatic salt energy storage," US20160298455A1, 2016
- [33] M. Albert, Z. Ma, H. Bao, and A. P. Roskilly, "Operation and performance of Brayton Pumped Thermal Energy Storage with additional latent storage," *Appl Energy*, vol. 312, Apr. 2022, doi: 10.1016/j.apenergy.2022.118700.
- [34] T. R. Davenne and B. M. Peters, "An Analysis of Pumped Thermal Energy Storage With De-coupled Thermal Stores," *Front Energy Res*, vol. 8, Aug. 2020, doi: 10.3389/fenrg.2020.00160.
- [35] F. Ni and H. S. Caram, "Analysis of pumped heat electricity storage process using exponential matrix solutions," *Appl Therm Eng*, vol. 84, pp. 34–44, Jun. 2015, doi: 10.1016/J.APPLTHERMALENG.2015.02.046.
- [36] L. Wang, X. Lin, L. Chai, L. Peng, D. Yu, and H. Chen, "Cyclic transient behavior of the Joule–Brayton based pumped heat electricity storage: Modeling and analysis," *Renewable and Sustainable Energy Reviews*, vol. 111, pp. 523–534, Sep. 2019, doi: 10.1016/J.RSER.2019.03.056.
- [37] Y. Q. Ge, Y. Zhao, and C. Y. Zhao, "Transient simulation and thermodynamic analysis of pumped thermal electricity storage based on packed-bed latent heat/cold stores," *Renew Energy*, vol. 174, pp. 939–951, Aug. 2021, doi: 10.1016/J.RENENE.2021.04.094.
- [38] A. Benato, "Performance and cost evaluation of an innovative Pumped Thermal Electricity Storage power system," *Energy*, vol. 138, pp. 419–436, Nov. 2017, doi: 10.1016/J.ENERGY.2017.07.066.

- [39] D. Salomone-González, J. González-Ayala, A. Medina, J. M. M. Roco, P. L. Curto-Risso, and A. Calvo Hernández, "Pumped heat energy storage with liquid media: Thermodynamic assessment by a Brayton-like model," *Energy Convers Manag*, vol. 226, p. 113540, Dec. 2020, doi: 10.1016/J.ENCONMAN.2020.113540.
- [40] L. X. Chen, P. Hu, P. P. Zhao, M. N. Xie, and F. X. Wang, "Thermodynamic analysis of a High Temperature Pumped Thermal Electricity Storage (HT-PTES) integrated with a parallel organic Rankine cycle (ORC)," *Energy Convers Manag*, vol. 177, pp. 150–160, Dec. 2018, doi: 10.1016/J.ENCONMAN.2018.09.049.
- [41] H. Zhang, L. Wang, X. Lin, and H. Chen, "Technical and economic analysis of Brayton-cycle-based pumped thermal electricity storage systems with direct and indirect thermal energy storage," *Energy*, vol. 239, Jan. 2022, doi: 10.1016/j.energy.2021.121966.
- [42] L. Wang, X. Lin, H. Zhang, L. Peng, X. Zhang, and H. Chen, "Analytic optimization of Joule–Brayton cycle-based pumped thermal electricity storage system," *J Energy Storage*, vol. 47, p. 103663, Mar. 2022, doi: 10.1016/J.EST.2021.103663.
- [43] H. Zhang, L. Wang, X. Lin, and H. Chen, "Combined cooling, heating, and power generation performance of pumped thermal electricity storage system based on Brayton cycle," *Appl Energy*, vol. 278, Nov. 2020, doi: 10.1016/j.apenergy.2020.115607.
- [44] L. Wang, X. Lin, H. Zhang, L. Peng, and H. Chen, "Brayton-cycle-based pumped heat electricity storage with innovative operation mode of thermal energy storage array," *Appl Energy*, vol. 291, Jun. 2021, doi: 10.1016/j.apenergy.2021.116821.
- [45] L. Wang *et al.*, "Unbalanced mass flow rate of packed bed thermal energy storage and its influence on the Joule-Brayton based Pumped Thermal Electricity Storage," *Energy Convers Manag*, vol. 185, pp. 593–602, Apr. 2019, doi: 10.1016/J.ENCONMAN.2019.02.022.
- [46] J. D. McTigue, P. Farres-Antunez, K. S. J, C. N. Markides, and A. J. White, "Techno-economic analysis of recuperated Joule-Brayton pumped thermal energy storage," *Energy Convers Manag*, vol. 252, Jan. 2022, doi: 10.1016/j.enconman.2021.115016.
- [47] H. Yang, J. Li, Z. Ge, L. Yang, and X. Du, "Dynamic characteristics and control strategy of pumped thermal electricity storage with reversible Brayton cycle," *Renew Energy*, vol. 198, pp. 1341–1353, Oct. 2022, doi: 10.1016/J.RENENE.2022.08.129.
- [48] G. F. Frate, L. Ferrari, and U. Desideri, "Techno-Economic Comparison of Brayton Pumped Thermal Electricity Storage (PTES) Systems Based on Solid and



- Liquid Sensible Heat Storage," *Energies (Basel)*, vol. 15, no. 24, p. 9595, Dec. 2022, doi: 10.3390/en15249595.
- [49] A. J. White, "Loss analysis of thermal reservoirs for electrical energy storage schemes," *Appl Energy*, vol. 88, no. 11, pp. 4150–4159, Nov. 2011, doi: 10.1016/J.APENERGY.2011.04.030.
- [50] J. D. McTigue, C. N. Markides, and A. J. White, "Performance response of packed-bed thermal storage to cycle duration perturbations," *J Energy Storage*, vol. 19, pp. 379–392, Oct. 2018, doi: 10.1016/J.EST.2018.08.016.
- [51] A. White, J. McTigue, and C. Markides, "Wave propagation and thermodynamic losses in packed-bed thermal reservoirs for energy storage," *Appl Energy*, vol. 130, pp. 648–657, Oct. 2014, doi: 10.1016/J.APENERGY.2014.02.071.
- [52] A. J. White, J. D. McTigue, and C. N. Markides, "Analysis and optimisation of packed-bed thermal reservoirs for electricity storage applications," *Proceedings of the Institution of Mechanical Engineers, Part A: Journal of Power and Energy*, vol. 230, no. 7, pp. 739–754, Nov. 2016, doi: 10.1177/0957650916668447.
- [53] A. Smallbone, V. Jülch, R. Wardle, and A. P. Roskilly, "Levelised Cost of Storage for Pumped Heat Energy Storage in comparison with other energy storage technologies," *Energy Convers Manag*, vol. 152, pp. 221–228, Nov. 2017, doi: 10.1016/J.ENCONMAN.2017.09.047.
- [54] Y. Zhao *et al.*, "Thermo-economic assessments of pumped-thermal electricity storage systems employing sensible heat storage materials," *Renew Energy*, vol. 186, pp. 431–456, Mar. 2022, doi: 10.1016/J.RENENE.2022.01.017.
- [55] Y. Zhao, M. Liu, J. Song, C. Wang, J. Yan, and C. N. Markides, "Advanced exergy analysis of a Joule-Brayton pumped thermal electricity storage system with liquid-phase storage," *Energy Convers Manag*, vol. 231, Mar. 2021, doi: 10.1016/j.enconman.2021.113867.
- [56] J. Gonzalez-Ayala, D. Salomone-González, A. Medina, J. M. M. Roco, P. L. Curto-Risso, and A. Calvo Hernández, "Multicriteria optimization of Brayton-like pumped thermal electricity storage with liquid media," *J Energy Storage*, vol. 44, p. 103242, Dec. 2021, doi: 10.1016/J.EST.2021.103242.
- [57] C. Lu *et al.*, "Dynamic modeling and numerical investigation of novel pumped thermal electricity storage system during startup process," *J Energy Storage*, vol. 55, p. 105409, Nov. 2022, doi: 10.1016/J.EST.2022.105409.
- [58] C. Willich, C. N. Markides, and A. J. White, "An investigation of heat transfer losses in reciprocating devices," *Appl Therm Eng*, vol. 111, pp. 903–913, Jan. 2017, doi: 10.1016/J.APPLTHERMALENG.2016.09.136.
- [59] S. Georgiou, N. Shah, and C. N. Markides, "A thermo-economic analysis and comparison of pumped-thermal and liquid-air electricity storage systems," *Appl*

- Energy*, vol. 226, pp. 1119–1133, Sep. 2018, doi: 10.1016/J.APENERGY.2018.04.128.
- [60] P. Farres-Antunez, J. D. McTigue, and A. J. White, “A pumped thermal energy storage cycle with capacity for concentrated solar power integration,” in *2019 Offshore Energy and Storage Summit, OSES 2019*, Institute of Electrical and Electronics Engineers Inc., Jul. 2019. doi: 10.1109/OSES.2019.8867222.
- [61] G. F. Frate, L. Paternostro, L. Ferrari, and U. Desideri, “Off-Design of a Pumped Thermal Energy Storage Based on Closed Brayton Cycles,” *J Eng Gas Turbine Power*, vol. 144, no. 2, 2022, doi: 10.1115/1.4052426.
- [62] M. Petrollese, M. Cascetta, V. Tola, D. Cocco, and G. Cau, “Pumped thermal energy storage systems integrated with a concentrating solar power section: Conceptual design and performance evaluation,” *Energy*, vol. 247, p. 123516, May 2022, doi: 10.1016/J.ENERGY.2022.123516.
- [63] R. Turton, R. C. Bailie, W. B. Whiting, J. A. Shaeiwitz, and D. Bhattacharyya, *Analysis, Synthesis, and Design of Chemical Processes Fourth Edition*. London: Pearson Education International, 2012.

